Copyright Warning & Restrictions

The copyright law of the United States (Title 17, United States Code) governs the making of photocopies or other reproductions of copyrighted material.

Under certain conditions specified in the law, libraries and archives are authorized to furnish a photocopy or other reproduction. One of these specified conditions is that the photocopy or reproduction is not to be "used for any purpose other than private study, scholarship, or research." If a, user makes a request for, or later uses, a photocopy or reproduction for purposes in excess of "fair use" that user may be liable for copyright infringement,

This institution reserves the right to refuse to accept a copying order if, in its judgment, fulfillment of the order would involve violation of copyright law.

Please Note: The author retains the copyright while the New Jersey Institute of Technology reserves the right to distribute this thesis or dissertation

Printing note: If you do not wish to print this page, then select "Pages from: first page # to: last page #" on the print dialog screen

ABSTRACT

IN VITRO EVALUATION OF HUMAN MESENCHYMAL STEM CELL NEURAL DIFFERENTIATION ON TYROSINE-DERIVED POLYARYLATES AND POLYCARBONATES

by
Yee-Shuan Lee

Present spinal cord injury treatments cannot restore motor and sensory functions caused by the injury. These functions can return in the hopes of repairing the neural cells with a tissue engineered designed scaffold complex. The scaffold complex will include cells to repair and replace the damaged cells.

Mesenchymal stem cells (MSC) are multipotent adult stem ells that are capable of differentiating along several lineage pathways. Neural stem cell and MSC differentiating along the neural lineage have been investigated both in vivo and in vitro depicting its feasibility. MSC for neural differentiation can be achieved by microenvironmental signaling. Substrate surface characteristics may influence both neuron and stem cell behavior and differentiation.

The effects of the polymer surface of tyrosine-derived polycarbonates and polyarylates on MSC differentiation along the neural lineage were investigated in this research. These polymers were developed by Dr. Joachim Kohn, where by altering the length of the alkyl ester pendent chain and the backbone composition, these polymers can have a gradual change in physicomechanical, chemical, and biological properties.

The MSC differentiated into neuron-like cell at 24 hours after induction. These cells express the presence of NSE which is a neuron marker. No systematic variation on cell proliferation among the polyarylate polymers was observed. The oxygen-contained diacid backbone stimulated cell growth on all the polyarylate polymers in this study. Cell proliferation increased as the substrate surface became less hydrophobic for all polymer

surfaces. Wettability of polycarbonate polymers depicts high linear correlation with cell number and percentage of neural differentiation. The copolymer of tyrosine-derived poly DTE carbonate and 5% PEG was hydrophobic and did not stimulate cell growth and cells tend to aggregate on this substrate surface.

IN VITRO EVALUATION OF HUMAN MESENCHYMAL STEM CELL NEURAL DIFFERENTIATION ON TYROSINE-DERIVED POLYARYLATES AND POLYCARBONATES

by
Yee-Shuan Lee

A Thesis
Submitted to the Faculty of
New Jersey Institute of Technology
In Partial Fulfillment of the Requirements for the degree of
Master of Science in Biomedical Engineering

Department of Biomedical Engineering

August 2005

APPROVAL PAGE

IN VITRO EVALUATION OF HUMAN MESENCHYMAL STEM CELL NEURAL DIFFERENTIATION ON TYROSINE-DERIVED POLYARYLATES AND POLYCARBONATES

Yee-Shuan Lee

Dr. Treena Livingston Arinzeh, Thesis Advisor — Date
Assistant Professor of Biomedical Engineering, NJIT

Dr. Michael Jaffe, Committee Member — Date
Research Professor of Biomedical Engineering, NJIT

Dr. David Kristol, Committee Member — Date
Professor of Biomedical Engineering, NJIT

BIOGRAPHICAL SKETCH

Author: Yee-Shuan Lee

Degree: Master of Science

Date: August 2005

Undergraduate and Graduate Education:

- Master of Science in Biomedical Engineering
  New Jersey Institute of Technology, Newark, NJ, 2005

- Bachelor of Science in Biomedical Engineering
  University of Southern California, Los Angeles, CA, 2002

Major: Biomedical Engineering

Poster Presentation:

Lee YS, Abbassi Y, and Arinzeh,
"The effect of piezoelectric material on human mesenchymal stem cell differentiation,"
7th Symposium of Biomaterials Science, New Brunswick, NJ, October 2004.

Participation, Anticipation, Determination

Define

My

Present

Mom, Dad, John

Define

My

Past, Present, and Future

ACKNOWLEDGMENT

I would like to take this opportunity to express my greatest appreciation to Dr. Treena Livingston Arinzeh, who is my thesis advisor, for her support, encouragement, and reassurance of my research.

I would like to thank Dr. Michael Jaffe and Seung-uk Yoo for their knowledge and support of analyzing the polymers in this experiment, which plays an important aspect of this research.

I would like to thank Dr. David Kristol for being part of my thesis review committee.

I would also like to thank my friends here who have provided great memories while I was finishing my thesis and all the help they provided.

TABLE OF CONTENTS

TABLE OF CONTENTS
(Continued)

LIST OF TABLES

LIST OF FIGURES

LIST OF FIGURES
(Continued)

CHAPTER 1

INTRODUCTION

1.1 Spinal Cord Injury

Spinal cord injury (SCI) is primarily defined as the loss of movement and sensation innervated from areas of the spinal cord below the site of injury. SCI is classified as either complete or incomplete SCI. Complete SCI is defined as the total loss of sensory and motor functions and incomplete SCI is defined as no total loss of sensory and motor functions. At the injury site, fractures and compression of the vertebrate can crush and destroy the axons. In the United States alone, there are approximately 247,000 people living with SCI and approximately 11,000 new cases annually [1]. Traditional approach has been secondary injury prevention to limit injury progression with neuroprotective agents. Thus, recovery of functional loss is limited. Survivors of SCI often develop complications such as chronic pain, bladder dysfunction, respiratory and heart problems [2]. Hence future therapy should be geared toward functional recovery.

Axonal transaction or axotomy is the separation of the cell body and distal segment of the axon by cutting or slowly by crushing as in a SCI [3]. The myelin sheath of the distal segment of the damaged axon will eventually break off and be enveloped by the phagocytic cells. This phenomenon is known as the Wallerian degeneration. The remaining proximal neural cell body may be killed by apoptosis or chromatolytic reaction. Chromatolytic reaction is the metabolic alternation caused by changing cellular signal mechanism that often resulted in neuron gene expression alternation. The synaptic function of the chromatolytic neurons could also be depressed because it is most likely to

be replaced by the gilial cells. Thus factors influence repairing strategy for axonal regeneration after SCI include: (1) replacing damaged axon, which should involve remyelination, bridging the proximal and distal end, and regenerating new axon, and/or (2) prevention of chromatolytic neurons and suppression of axonal growth.

Suppressing neurite extension inhibitor and using scaffolds with growth factors to bridge the gap at the injury site are the major factors for repairing SCI [4]. Transplanting cells to bridge the gap at the injury site and remyelination of injured axons have been investigated previously [5-8] but does not show complete functional recovery. Stem cell technology may be able to provide better means of repairing dysfunction cells. Mouse embryonic stem cells have shown successful regeneration of myelinated axons in animal model and may be a treatment option for primary and secondary demyelinating diseases [9]. Neural stem cells in the brain are capable of differentiating into neurons, astrocytes, and oligodendrocytes. Neurons are responsible for transmitting nervous signals and the presence of astrocytes and oligodendrocytes aid the signal transfer process.

Neural stem cell and mesenchymal stem cell are able to differentiate along the neural lineage both in vivo and in vitro for the purpose of repairing spinal cord injury [7-12] and can be restricted to one neural cell type [13-16]. Various scaffolds were developed for tissue regeneration at cavity formation site after spinal cord injury [16]. Fabrication of scaffolds with nerve growth factors [17,18] and surface etching techniques [19] were to direct and enhance neural cell regeneration. Self-assembling peptide scaffolds have shown active synapses of rat neuron and support cell attachment, differentiation, and neurite outgrowth [20]. Poly(lactic-co-glycolic acid) (PLGA) and PLGA-polylysine scaffolds seeded with murine neural stem cells have shown promise as

scaffolds in SCI treatment in rat models [21]. Designed uniaxial linear pores agarose scaffolds were fabricated to guided neurite growth [22]. Porous nano-fibrous PLLA scaffold supported neural stem cells differentiation and structure cue for neurite outgrowth [23]. Scaffold is essential in long distance axonal regeneration as it acts as a bridge for axonal extension. Optimized design of scaffolds in combination with stem cell technology may lead to possible tissue engineering treatments.

1.2 Tissue Engineering

Contemporary medicine is targeted for two goals: (1) to prevent and/or control the disorder and (2) to restore lost tissue and cellular function. Traditional surgical therapies for dysfunction tissue involve repair, replacement, reconstruction, and removal. Typical repair method involves stitching at the injury site that often accompanied by scar formation. Replacement of tissue from autologous, allogeneic, and xenogeneic source has been practiced but immune response is the primary concern for the latter two sources. Replacing dysfunction heart valves with porcine heart valves and burnt skin with skins from other area of the body are some examples of tissue replacement. Reconstruction with an alternative tissue type from our body may reduce immune response but can limit functional recovery. If none of the choice above may be considered, the dysfunctional tissue will be removed and often replaced with prosthesis. Via traditional treatment, the damaged tissues are not regenerated and often aim to slow down further tissue damage. For example, if a young patient required a total knee replacement, the likelihood of having a replacement later is very high due to the wear of the prosthesis components and

the growth of the child. Hence functional replacement and repairing are essential for ideal recovery.

Tissue engineering is a multi-disciplinary study involves primarily biology, material science, manufacture, medicine, and engineering to develop functional biological substitutes that can repair, maintain, or improve function of the damaged tissue [24]. The idea of tissue engineering is to mimic biological mechanisms and environment to promote repairing of damaged tissue. Scaffolding materials i.e. biodegradable polymers are constructed into shapes as needed and then seeded with cells and growth factors or others that will promote proliferation. While the cells proliferate, they will grow into a three-dimensional shape based on the scaffold structure. The scaffold should decompose gradually and the surrounding cells will blend in with the regenerated tissue structure and thus repaired the damaged tissue.

Three aspects need to be considered for a tissue engineering application: (1) *Cell selection*. This is critical for a successful cellular and tissue regeneration. Earlier stage, the mature cell were used directly for repairing. Later on involvement of stem cell technology has brought new choices for cell selection. (2) *Scaffold*. The purpose of the scaffold is to create a biological environment mostly similar to the extracellular matrix (ECM). The scaffold should at least allow the selected cells to attach and proliferate. In advance term, it should also promote stem cell differentiation if stem cell is the cell source and also reduce the inhibition triggered by the body for restraining regeneration. (3) *Proper signal and cue*. Cell continuously go through cell cycle. Mature cells eventually die and replaced by new cells. Signals such as receptor proteins and hormone are released in the ECM and controls the cell cycle by various signaling mechanisms.

Optimizing the combination of cells, scaffolds, and signals may create a suitable environment for tissue regeneration in vivo and in vitro.

Cells are organized in the extracellular matrix (ECM) which is mostly composed of proteins and glycosaminoglycans cross-linked network that controls and regulates all cell-related activities such as cellular adhesion, protein binding sites, and degradation. To allow tissue repair, scaffolds are used for initial cell attachment and promote cell growth as similar to the ECM. Thus surface properties of the scaffold are important for initial cell attachment. A scaffold should be biocompatible and has controlled biodegradation rate as it is gradually being replaced by new functional cells and healthy surrounding cells. Interconnected porous structure may also help in cellular growth and communication.

Two component of the scaffold should be considered, the polymer composition and the geometric structure. The polymer composition defined the chemical and physical properties of the scaffold. The bulk property of the scaffold such as stiffness should provide the mechanical support at the site in our body and the surface property should at least allow good cell-polymer interactions. The geometric shape can be determined by the fabrication method. Fiber mesh, phase separation, solvent casting and particulate leaching, polymer/ceramic fiber composite foam, and nano-spinning are some example of fabrication methods. The geometric shape of the scaffold may influence stem cell differentiation where cell orientation was found to influence differentiation significantly [23]. Therefore optimizing the scaffold is essential for a successful cellular reconstruction.

1.3 Polymers

Polymers, either natural occurring or synthetic have utilized for a wide range of medical application because of its availability and manufacturing feasibility. Poly (methyl methacrylate) (PMMA), poly (lactic acid) (PLA), poly (glycolic acid) (PGA) and poly (L-lactic acid) (PLLA) are some examples of FDA approved polymers for biological applications. In drug delivery and tissue engineering applications, special designed biodegradable polymers may optimize the performance.

1.3.1 Biodegradable Polymers

Biodegradable polymers are mostly used for extended release drug delivery to allow better delivery targeting and more user-friendly. Biodegradable suture material and pins are popularly used for tissue repairing. In tissue engineering, scaffolds are implanted into the body for cell and tissue repair and regeneration. Biodegradable polymers hence are thought to be promising for tissue engineering application. The selected scaffolding polymer should not degrade before the tissue is repaired yet at the same time should not produce cytotoxic by-products after degradation. Recent selection criteria for a suitable scaffolding material does not only have to be biocompatible and stable for its application, but it should at least support new tissue growth, prevent cellular activity and growth such as lesion, guide tissue response and reduce immunologic problems, and enhance scaffold-host interaction [25].

Biological derived polymers such as type I collagen, chitosan, glycosaminoglycans, polyhyseoxyalkanoates have been used for scaffold fabrication and have studied widely for various applications. Synthetic poly(amino acid) has been

investigated for many years due to its non-toxic by-product after degradation and the variability of composition due to its side chain attachment. However, very few has been developed for application due to its poor mechanical strength and very limited processibility cause by its amide backbone, where strong hydrogen bond linkage makes it insoluble [27]. The insoluble linkage restricts the feasibility of processing and increases the cost if undergoes a massive production. In addition, poly(amino acids) also creates immunological responses. Therefore, innovation of pseudo-poly(amino acid) was introduced by eliminating the amide backbone resulting increase of processiblity and improves the mechanical properties [26,27]. The polymers used in this study are from a family of tyrosine-derived polycarbonates and polyarylates developed by Dr. Joachim Kohn at Rutgers University.

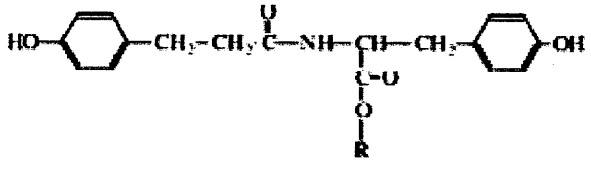

Figure 1.1 Structure of desaminotyrosul-tyrosin alkyl ester [26].

Tyrosine is a naturally occurring protein. Hence they will not produce cytotoxic by-products after degradation. The amino acids are polymerized by using the functional group to produce the non-amide bonds [28]. Protecting groups were attached to the carboxyl and amide ends of the tyrosine to prevent dipeptide bonds [26]. The protecting step was later defined by replacing one tyrosine with desaminotyrosine and creating the final backbone structure, desaminotyrosyl-tyrosine alkyl ester for tyrosine-derived polymers (Figure 1.1). This structure is a key element in the mechanical properties and manufacture feasibility of this polymer [26].

1.3.2 Tyrosine-derived Polycarbonates

Tyrosine-derived polycarbonates are homopolymers of desaminotryrosyl-tyrosine alkyl ester (Figure 1.2). The structure and properties is further characterized by the alkyl ester, which is the "R" group in Figure 1.2 and is usually the ethyl, butyl, hexyl, or octyl ester pendent chains. They are generally referred as poly(DTE carbonate), poly (DTB carbonate), poly(DTH carbonate), poly(CTO carbonate) respectively [28]. Additional choices of pendent chain such as methanol, Dondeccanol, berzyl alcohol, 2-(2-Ethoxyethoxy) ethanol have also been evaluated [29].

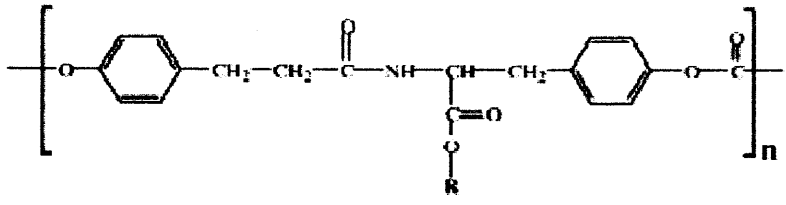

Figure 1.2 Structure of tyrosine-derived polycarbonates [26].

Average molecular weight range from 120,000 to 450,000 Da due to the size of the alkyl ester pendent chain [28]. All tyrosine-derived polycarbonates are amorphous and have low glass transition temperatures and a high degree of thermal stability. The pendent chain influences the transition temperature, solubility, ductility, tensile strength, and contact angle significantly. Increase in pendent chain size is expected to increase the free volume of the polymer [28]. Altering the free volume of the polymer will also change the mobility and bond interaction. Strong interchain hydrogen bonds were found to be reducing solubility and ductility [27]. Therefore increasing the pendent chain size will reduce the strength of the interchain hydrogen bonds leading to an increase in solubility and ductility. In another word, the polymer becomes more hydrophobic.

Increase in pendent chain size will allow more free volume and weaker interchain bonds hence lowering the glass transition temperature.

Cell attachment is essential for cell proliferation and differentiation and has found to be very depended on the wettability, which can be estimated by the water contact angle of the polymer surface. The polycarbonates have contact angles ranging from 73 to 90 where most cells favor in the range from 60 to 100 [28]. The wettability will decrease as the pendent chain length increases due to longer hydrocarbon chains [29]. Increase of hydrocarbon chains will increase the nonpolar characteristics on the surface and provide a better shielding on the polar ester and amide groups [29].

1.3.3 Tyrosine-derived Polyarylates

Tyrosine-derived polyarylates are copolymers with alternating A-B units [29]. Monomer A is tyrosine-derived diphenols and is the reactive group for pendant chain(R) attachment. Monomer B is aliphatic diacids which allows systematic variation in the backbone structure (Y) (Figure 1.3.3). Often used pendant chain group are methyl, ethyl, butyl, hexyl, and octyl which is similar to the polycarbonates. The diacids are generally succinic, glutaric, diglycolic, adipic, and sebacic acid that vary in oxygen-contained and length.

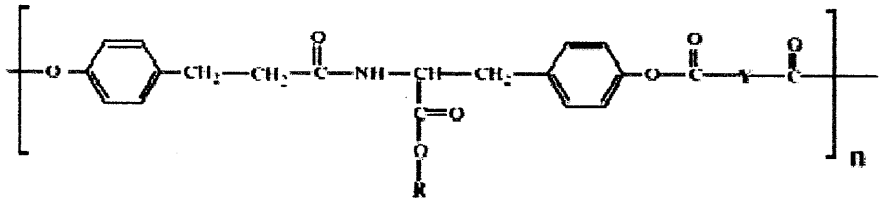

Figure 1.3 Structure of tyrosine-derived polyarylates [26].

Average molecular weight ranges from 50000 to 150000 g/mol [29]. The variation of R and Y exhibits predictable changes in glass transition temperature, surface wettability and cellular response [29]. Increase in methylene group in either pendant chain or backbone will increase the contact angle and decrease the glass transition temperature. Glass transition temperature is more sensitive to the backbone alternation than in the change of pendant chain. Cell proliferation is less influenced by the hydrophobicity of the surface because cells favor its oxygen-containing diacids in the backbone.

1.3.4 Tyrosine-derived Polycarbonate Containing PEG

These polymers were developed for applications in drug delivery, wound healing and artificial skin scaffolds, and degradable membranes where hydrophilic and fast degrading biomaterial is desired. The tyrosine-derived diphenolic monomer was copolymerized with poly(ethylene glycol) (PEG) and the product is characterized by the mole fraction percent of PEG, average molecular weight of PEG blocks, and the pendent alkyl group (Figure 1.4) [26]. PEG content variation influences the polymer properties significantly [30]. Increase in PEG content will decrease the glass transition temperature exponentially. At low PEG content, the polymers depict similar mechanical properties to the tyrosine-derived homopolymers. Increase in PEG content will reduce the stiffness and strength of the polymer. Increase in PEG content will also increase water uptake and degradation rate significantly. Copolymer with 5% or more PEG content will reduce cell attachment and proliferation notably reflecting its change in surface properties.

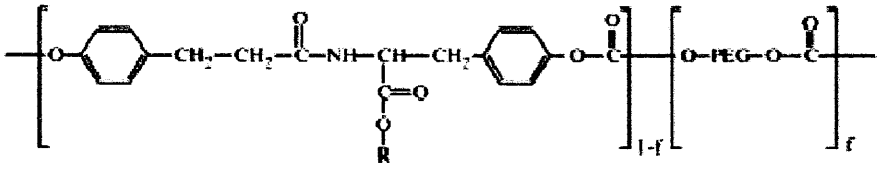

Figure 1.4 Structure of copolymer of tyrosine-derived polycarbonate and PEG [26].

1.3.5 Applications

Stable thermal properties and high solubility in various organic solvent of polycarbonates and polyarylates allow them to be processed in conventional polymer fabrication techniques such as extrusion, compression and injection molding, and solvent casting. This benefits the scaffolds fabrication for tissue engineering applications.

Tyrosine derived polycarbonates been developed as a biodegradable polymer for orthopedic applications. Poly(DTH carbonate) pins have shown better hard and soft tissue response compare to polydioanone (PDS) [31]. Poly(DTH carbonate) pins has low-grade foreign body response in muscle tissue and shown better implant and bone direct contacts. On the other hand, PDS showed minor immune response in muscle tissues and shown fibrous capsulation since implanted [31].

Tyrosine derived polyarylates are predominately used for scaffold fabrication due to its systematic characteristic. Osteogenic differentiation of mesenchymal stem cell on polyarylates have been evaluated and most hydrophilic surface demonstrated highest cell proliferation rate and most hydrophobic surface demonstrated highest osteogenic differentiation rate [32,33].

1.4 Stem Cell

Stem cells are unspecialized cells that are self-renewable for a long time via cell division. When stem cells are under certain conditions, they are capable of inducing into specific cell type such as heart, muscle, ligament, tendon, and neuron. Initially it was thought only embryos have stem cells. Embryonic stem cells are a small group of inner cell mass which is developed in an embryo when it is only couple days old. These cells are pluripotent and are capable to develop into all cell types that are necessary for fetal development. Embryonic stem cells are able to differentiate into all cell lineages and do not have plasticity limitation. This characteristic is ideally suitable for cellular genetic manipulation studies and may be feasible for tissue regeneration [34]. Later on, human embryonic stem cell was studied and found similarity to the mouse embryonic stem cells and may have great potential for tissue engineering [35]. However, the ethic issue of primate embryonic stem cell has limited the development of clinical application and research.

Multipotent stem cells can differentiate into less cell types and have limited plasticity compare to embryonic stem cells. Although multipotent stem cells may not provide as many potential as embryonic stem cells but the ethic issue can be avoided. Adult stem cells are multipotent and can differentiate into various lineages when provided appropriate microenvironment. Adult stem cells have been identified for many tissue types such as hematopoietic, neural, muscle, endothelial, and mesenchymal cells. Mesenchymal stem cells (MSC) are located in the bone marrow of adults hence is also known as the bone marrow stromal cells. These cells have been demonstrated to have the ability to differentiate into various connective tissue cell types such as osteocytes,

chondrocytes, myoblasts, fibroblasts, and possibly adipocytes and neurons [36,37]. Directing stem cells to differentiate into various lineages can be achieved by two methods: genetic manipulation and microenvironment control.

Genetic manipulation of embryonic stem cell and bone marrow stromal cells has been demonstrated for inducing differentiation along the neural lineage [38,39]. Mouse and human embryonic stem cells have been demonstrated to be able to differentiate into neural lineage by exposing to high concentration of retinoic acid [34,40-43]. Human mesenchymal stem cells are also able to differentiate into neural lineage by exposing to high concentration of retinoic acid [44] and with additive growth factors [45,46]. Induction media basis of β-mercapoethanol (BME) in serum-DMEM followed by 2% dimethylsulfoxide (DMSO), 200μM butylated hydroxyanisole (BHA) in serum free DMEM also induced the mesenchymal stem cell to differentiate into neural linage generally in a shorter time period [47-50]. Differentiation along the neural lineage was also observed after 6 days when the cells were treated with 0.5 mM isobutylmethylxanthine (IBMX) and 1 mM dibutyrul cyclic AMP [51]. The differentiated MSC showed immunofluorescent expression in neuron-specific enolase (NSE), tau, NeuN, neurofilament-M, GFAP, neuron-specific tubulin III (TuJ-1), nestin, MAP2 and synaptophysin. Electrophysiology tests were conduct to eliminate any false morphology where most of differentiated neuron-like cells show functional responses.

Not until long ago, people have thought neurons are not being regenerated in our body. However, it was discovered that there are small amount of neural stem cells that will differentiated along the neural lineage when it is needed [52]. In biological environment, the stem cells are regulated by chemical signal mechanisms to undergo

differentiation. It has also been observed that cellular attachment and cellular orientation may affect the stem cell behavior without the signals [23,53]. Alternately, the goal of optimizing the method for inducing MSC along the neural lineage is to provide possible choices for neuron regeneration. An optimized composition of scaffold and differentiation method is essential for neural repair. Promoting neural differentiation of MSC on scaffolding materials have been studied [54]. Scaffold material composition and structure should be investigated further to optimize MSC to differentiate along the neural lineage.

CHAPTER 2

RESEARCH OBJECTIVE

This research is to evaluate the effects of polymer substrate to mesenchymal stem cell differentiation along the neural lineage. The objectives of this research can be summarized as below to:

1. Polymer fabrication and characterization
2. Optimize MSC neural differentiation and characterization
3. Study the effects of proliferation and neural lineage differentiation of mesenchymal stem cell on various polymers based on wettability

CHAPTER 3

EXPERIMENTAL METHODS

3.1 Polymer Preparation

Polymers were prepared by the solvent casting method for 96-well polypropylene culture plates and spin casting method for 24-well polystyrene culture plates.

Solvent casting method was adapted from earlier techniques [28] where 1% wt/vol polymer was dissolved in methylene chloride. The solution was filtered with 0.45μm syringe filter (Fisherbrand, Pittsburgh, PA) and 300μL was applied to each well. The plate was air dried at room temperature for at least 48 hours prior of use in the chemical hood.

Spin casting method was adapted from earlier techniques [28]. Glass slides were cleaned by sonication twice each in 25%wt/vol of sodium hydroxide aqueous solution, 25% vol/vol of hydrochloric acid aqueous solution for 10 minutes and twice in 2% vol/vol of detergent aqueous solution for 30 minutes. Slides were then rinsed with distilled water followed by sonication each twice in 100% ethanol and methylene chloride for five minutes. Poly (styrene-silane) coating was applied to allow better adhesion of polymer solution to the surface by sonication twice in 2.5% wt/vol poly (styrene-silane) in ethyl acetate for five minutes. The glass slides were then lay out on glass plates and placed in a 60°C vacuum oven for 48 hours.

The glass slides were cooled preceding incubation period and was rinsed twice with ethyl acetate and methanol and dried in aluminum foil for 30 minutes. The glass slides were spin cast once with 2.5% wt/vol polymer solution in methylene chloride at

2000 rpm for 20 seconds (Headway Research, spin-coating apparatus). The glass disks were fixed to the 24-well plates by applying few drops of methylene chloride before placing the disks into the well. The plate was air dried at room temperature for at least 48 hours prior usage in the chemical hood.

3.2 Polymer Characterization

Raw and processed polymers were characterized by Thermogravimetric analysis (TGA) and Differential Scanning Colorimetery (DSC) techniques to verify any structural changes of the polymer and the absence of methylene chloride due to the process. The water contact angle was also evaluated to determine the relative wettibility and roughness of substrate surface.

TGA monitors the weight change of a material as a function of temperature under a controlled environment to measure thermal stability and composition. TA Instrument model Q50 TGA was used for this study and its weight change sensitivity is up to 1μg. Approximately 5mg of each polymer before and after processing was used. The samples were heated to 400 °C by an increment of 10°C per minute.

DSC measures the temperatures and heat flows of a material during thermal transitions (endothermic and exothermic reactions). Properties such as glass transition, crystallization, phase changes, melting, curing, stability, and oxidative stability can be determined. TA Instrument model Q100 was used for this study and thermal detection sensitivity is up to 1 microwatt. Approximately 5 mg of each polymer before and after was used and were evaluated by a heat-cool-heat cycle. The technique heated the sample

from -20°C to 250°C and cooled to -20°C then heated again to 250°C with a 10°C per minute temperature change.

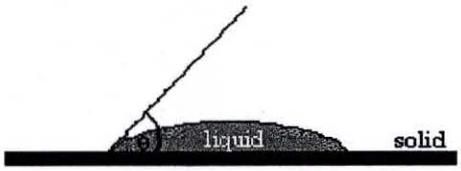

Figure 3.1 Defining contact angle [55].

Contact angle is the geometric angle formed by a liquid on a solid surface at the three phase boundary as shown in figure 2.1 and it quantitatively describes the solid wettibility of the liquid. Generally, for more hydrophobic surfaces, hydrophobic liquid was used and for more hydrophilic surfaces, hydrophilic liquid was used. Water is a hydrophilic substance and when used as the liquid for measuring contact angle, it is generally known as the water contact angle where higher angle value indicates a more hydrophobic surface. In this study, the water contact angles were measured by contact angle goniometry. 10μL of water was dropped on to the surface of the polymer located on a stage with a light source and a camera. An image was capture and the water contact angle was measured using Image J. This angle is also known as the advancing angle.

3.3 Cell Preparation

Human mesenchymal stem cells were obtained from adult bone marrow using previously published protocols [56]. Briefly, Bone marrow purchased from Cambrex Inc. was obtained from healthy human donors and by routine iliac crest aspiration. The bone marrow was washed and centrifuged to create density gradient fraction. The low density

mesenchymal stem cell – rich fraction was collected and incubated at 37°C in a humidified environment with 5% CO_2 in control media. The control media was replenished every 3 to 4 days until the culture become subconfluent. The mesenchymal stem cells were then detached with 0.25 trypsin in 1mM EDTA for 2 to 5 minutes at 37°C and subsequently replated or cryopreserved with 10% DMSO and 90% FBS as needed.

3.4 Media Preparation

The media used were prepared as previously described [54]. Two media were used for neural induction and one as control media. **Control Media**: The control media contains 20% fetal bovine serum (FBS) (Gibco, Carlsbad, CA), 1% antibiotic antimycotic, and low-glucose Dulbecco's Modified Eagle Media (DMEM). **Pre-Induction Media**: The pre-induction media contains 20% FBS, 10ng/mL basic Fibroblast Growth Factor (bFGF, Invitrogen, Carlsbad, CA), 1% antibiotic antimycotic, and DMEM. **Induction Media**: The Induction Media contains 200 μM butylated hydroxyanisole (BHA, Sigma-Aldrich, Saint Louis, MI), 10 μM forskolin (Sigma-Aldrich, Saint Louis, MI), 1 μM hydrocortisone (Sigma-Aldrich, Saint Louis, MI), 2 mM valporic acid (2-propylpentanoic acid, Sigma-Aldrich, Saint Louis, MI), 5 μg/mL insulin (Sigma-Aldrich, Saint Louis, MI), 25mM potassium chloride (KCl, Sigma-Aldrich, Saint Louis, MI), 1% antibiotic antimycotic, 2% dimethylsulfoxide (DMSO), and DMEM. All induction media were prepared on the day of usage.

3.5 Cell Culturing and Neuron Induction

Cell seeding density was varied from 1000cells/cm^2 to 6000 cells/cm^2 initially to achieve optimal differentiation. Induction media was initially using retinoic acid [44] and yielded immature neurons. Later the induction media was changed as described in Section 3.4.

All plates were exposed to UV light for 30 minutes for sterilization. All wells were pre-conditioned with control media for 24 hours prior seeding. Cryopreserved human mesenchymal stem cells (passage 2) were thawed and seeded at 4000 cells/cm^2 in all wells and cultured with the following steps:

1. Incubated with control media for 24 hours
2. Incubated with pre-induction media for 24 hours
3. Incubated with induction media for 24 hours

All cells were cultured with medium at a volume-to-surface ratio of 0.3. Cells were rinsed with PBS once between each change of medium. The control group was seeded on polystyrene tissue culture plates and followed the same time line of changing media but with control media only.

3.6 Immunochemistry

Immunocytochemical staining was used to examine neuron specific enolase (NSE) expression of the mesenchymal stem cells 24 hours after the induction. The cells were prepared as previously described [54]. Briefly, the cells were washed with PBS and fixed with 4% paraformeldehyde followed by cell permeabilization with 0.1% triton-x for 10 minutes each at room temperature. Subsequently, the cells were rinsed twice with 0.5 mg/mL sodium borohydride and incubated with 5% goat serum for 1 hour at room

temperature for blocking non-specific antibody binding. The cells were then incubated with 1:300 rabbit anti-human NSE antibody (Polyscience Inc., Warrington, PA) for 1 hour at 37°C followed by 1:100 goat anti-rabbit IgG antibody with TRITC conjugated (Sigma, Saint Louis, MI) for 40 minutes at 37°C. The cells were lastly incubated with 1:100 Fluorescein-Phalloidin (Molecular Probe, Carlsbad, CA) for 40 minutes at 37°C. The cells were rinsed with PBS twice and stored in anti-fade solution of 0.5mM ascorbic acid in 50% glycerol in PBS.

3.7 Neuronal Differentiation and Cell Proliferation Characterization

Cell morphology and NSE expression were examined by an inverted florescent microscopy with digital camera attachment. The model used in this study is Nikon Eclipse TS100 and DXM1200F with image processing software MetaVue 6.2r4. Quantification of neuronal differentiation was based on 4 random non-overlapping fields (x20) of each well. Each polymer has 4 wells each in induction and control group. The percentage of neuron-like cells were calculated based on the number of cells expressing NSE and neuron-like morphology.

DNA content is directly proportioned to the cell number. Therefore cell proliferation can be estimated indirectly by measuring DNA content in a sample. Picogreen ® dsDNA reagent (Molecular Probe, Carlsbad, CA) is a fluorescent nucleic acid stain to quantify double strand DNA in solution. The standard curve was established by measuring DNA content of calculated cell number solutions. The fluorescent absorbance reading from fluorometers or fluorescence microplate reader of the DNA containing solution of the sample can determine the DNA concentration from the

standard curve. In this study, DNA content was measured 24 hours after induction and Picoflourometer from Turner Designs, model 8000-003 with blue light emission was used.

Statistical analysis was performed to evaluate the statistical significance of various scaffold polymers on cell proliferation and neural differentiation. One way analysis of Variance (ANOVA) and Tukey-Kramer test were performed to test between groups ($p<0.05$).

CHAPTER 4

RESULTS

4.1 Polymer Characterization

4.1.1 TGA and DSC Test Results

TGA and DSC are thermal analysis methods to confirm the absence of methylene chloride in the polymer film. All TGA and DSC results for each polymer before and after processing are presented in Appendix A and B, respectively.

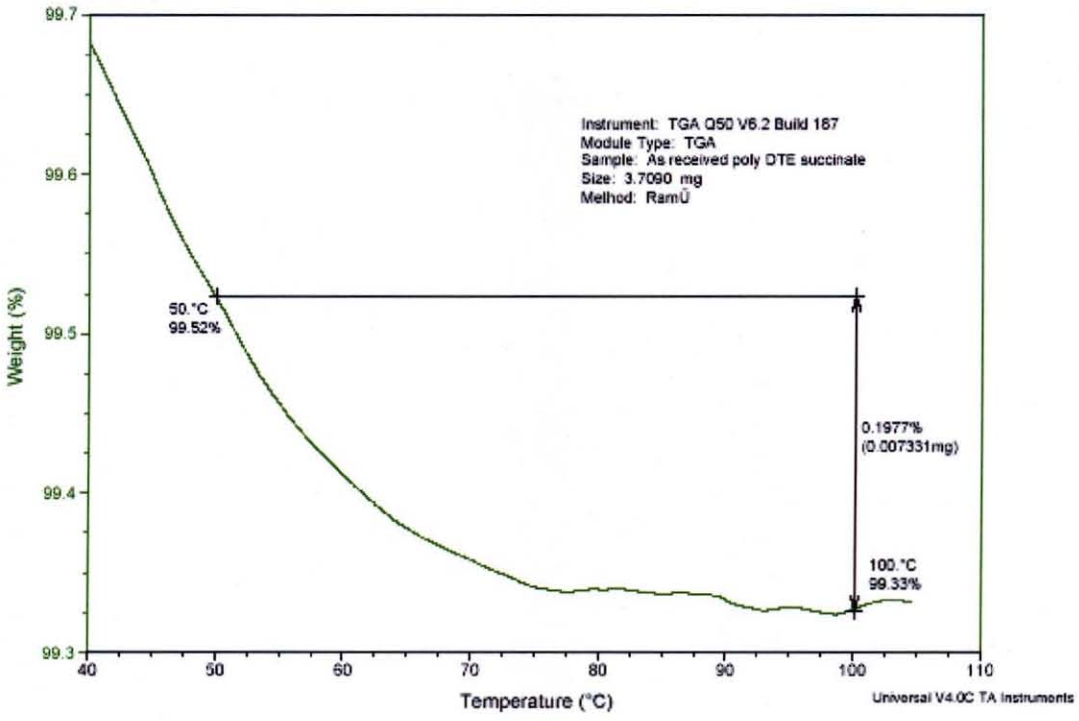

Figure 4.1 TGA result of poly DTE succinate as in received form.

TGA results show weight loss of the polymer over a range of temperatures. If methylene chloride was presented in the polymer film, a large weight loss should occur when the solvent starts to evaporate. The absence of methylene chloride could be

observed by a weight loss less than 1%. The TGA result for Poly DTE succinate as received showed a 0.1977% weight loss (Figure 4.1). This small weight loss may due to water vapor and is considered insignificant. The TGA results of poly DTE succinate in film showed a weight loss of 0.2719% (Figure 4.1). It has a slightly greater weight that loss the as received polymer possibly due to the methylene chloride in the polymer film. All polymers films showed a weight loss less than 1% and hence methylene chloride is negligible in the polymer films.

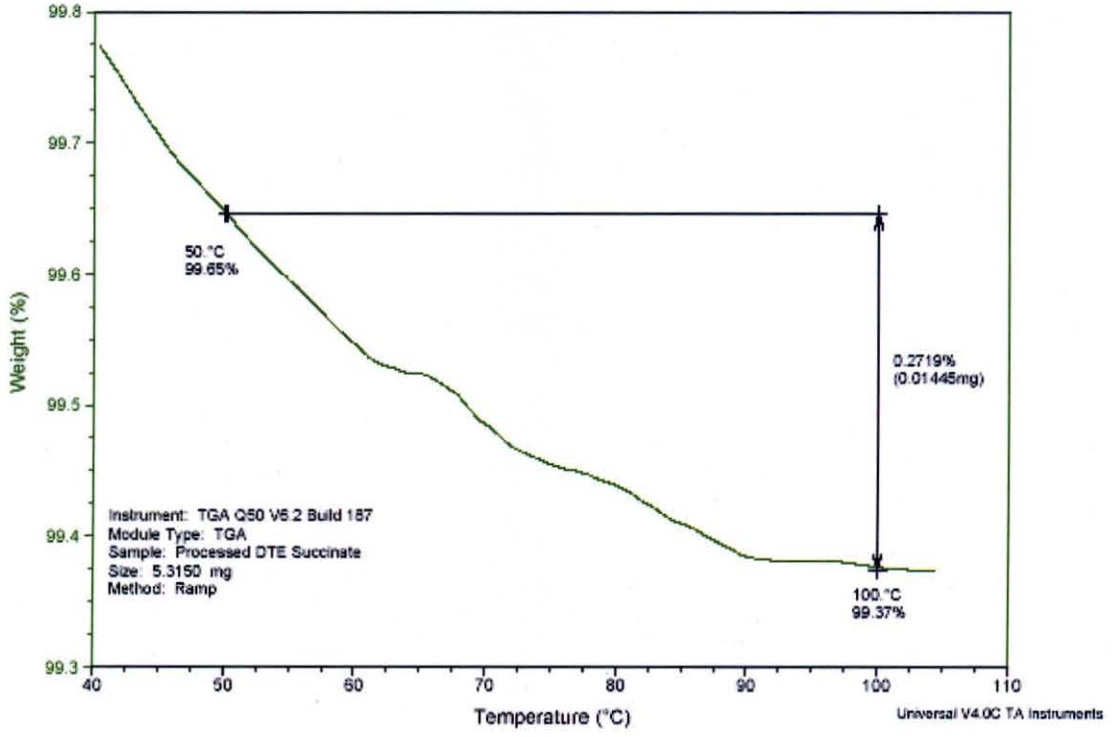

Figure 4.2 TGA result of poly DTE succinate in processed form.

Crystallization point was not observed in the DSC results hence demonstrating the polymers were amorphous. The transition temperature (T_g) of poly DTO carbonate before processing was 52.92°C (Figure 4.3) and after processing was 52.91°C (Figure

4.4). The small difference in (T_g) depicts the processing method does not alter the thermal property of the polymer. This applies to all of the polymer films.

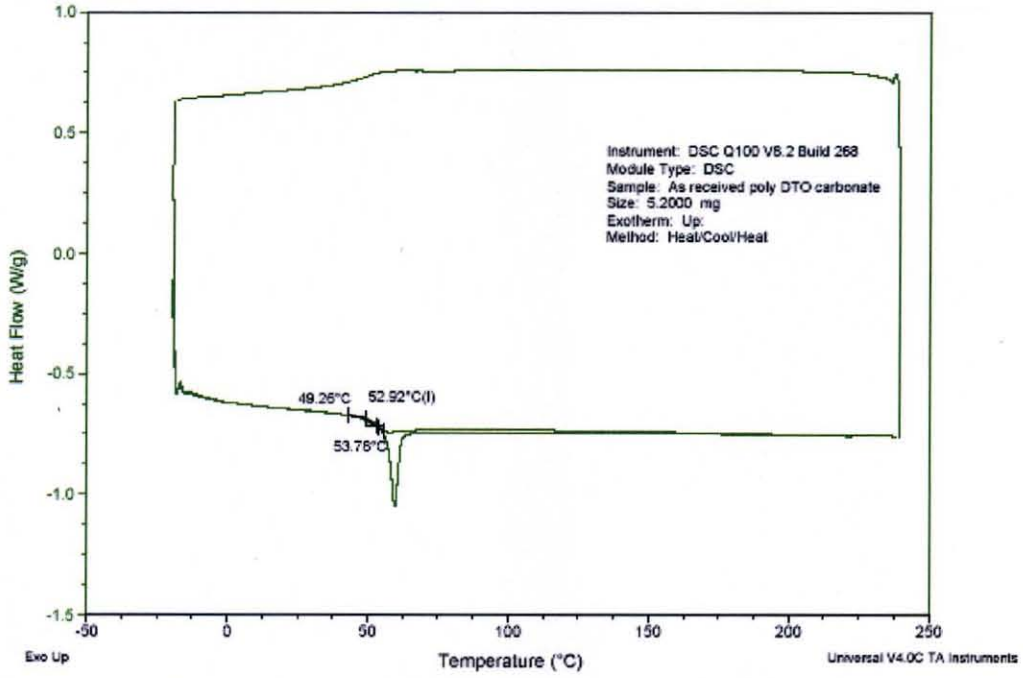

Figure 4.3 DSC result for poly DTO carbonate in received form.

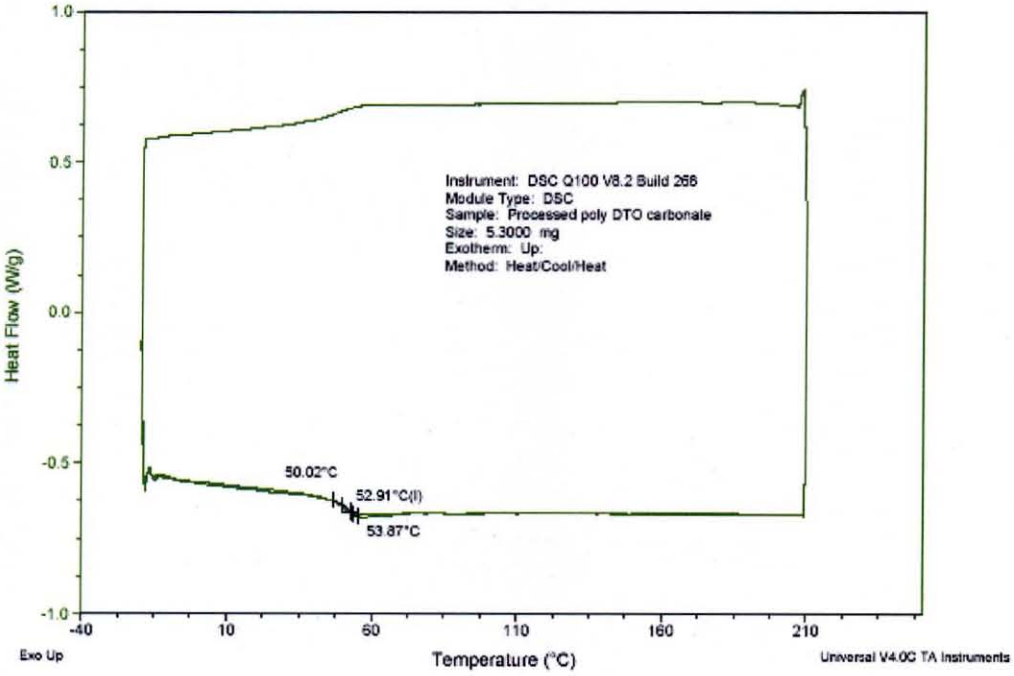

Figure 4.4 DSC result for poly DTO carbonate in processed form.

4.1.2 Water Contact Angle Results

The water contact angle quantitatively describes the wettability of the polymer. From Table 4.1, the surface of the DTO polysebacate is the most hydrophobic among the six polymers and DTE carbonate is the least hydrophobic surface. The copolymer of DTE carbonate and 5% PEG has the second most hydrophobic surface compared to the hydrophilic surface of DTE carbonate. It showed that polymer composition can significantly influence on the surface property.

Table 4.1 Polymer Water Contact Angle

Poly carbonates			Poly sebacate		Poly succinate
DTE	DTO	DTE-5% PEG	DTE	DTO	DTE
69.759	80.783	86.155	76.151	86.571	73.370

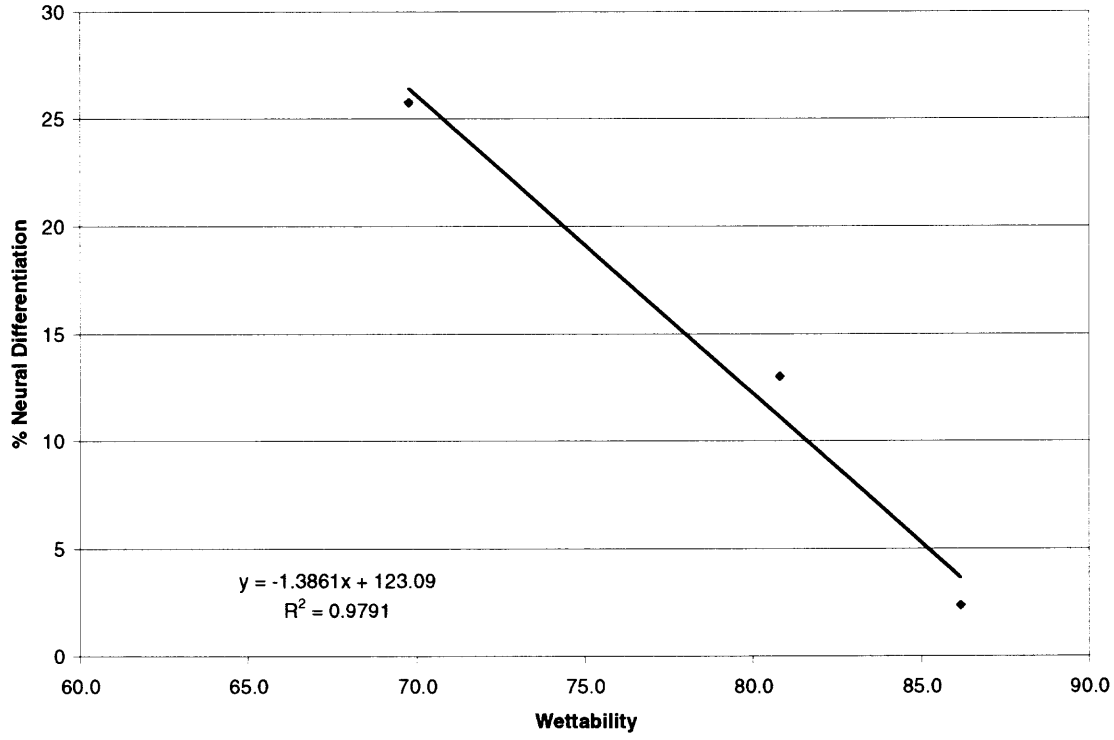

Figure 4.5 Percentage of neural differentiation vs. wettability for polycarbonates.

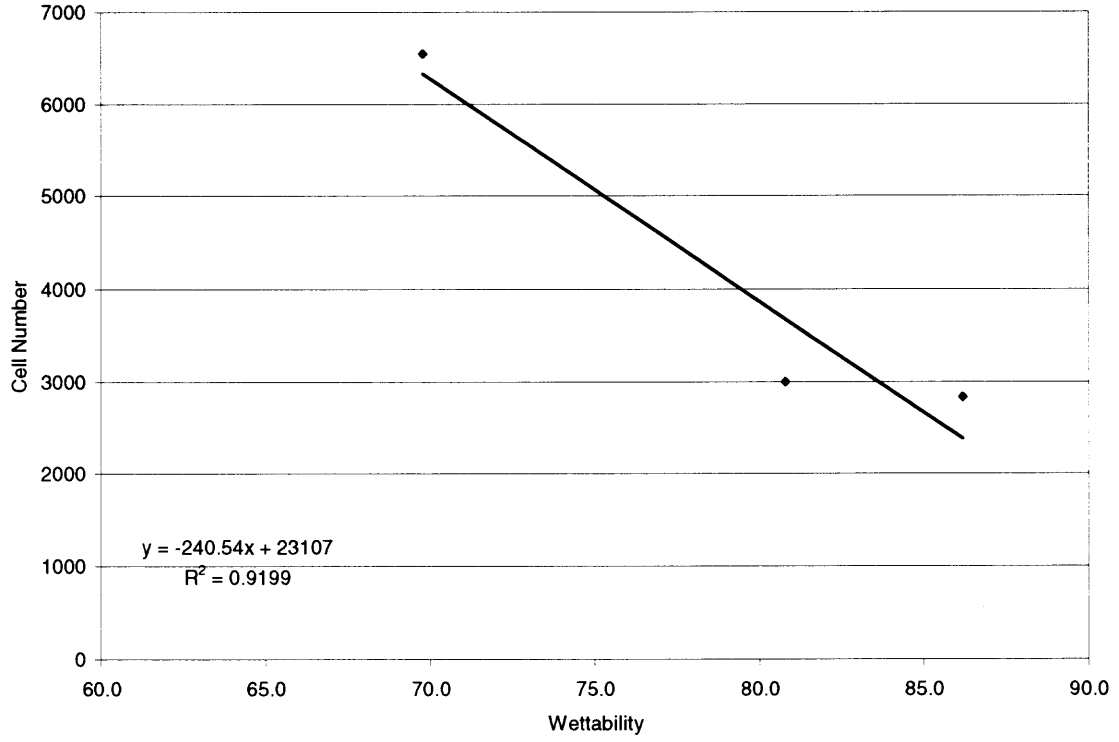

Figure 4.6 MSC number in control group vs. wettability for polycarbonates.

The percentage of neural differentiation (Figure 4.5) and MSC proliferation (Figure 4.6) of the polycarbonates polymers were linearly related to the wettability of the polymer surface. As the surface became more hydrophobic, the cell number and neural differentiation percentage decreased. MSC proliferation was less linear correlated to the wettability of the surface than MSC differentiation.

4.2 Cell Number

DNA assay was used to evaluate cell proliferation on each polymer surfaces. In Figure 4.7, the polyarylates generally have higher cell numbers in both control and induction group as compared to the polycarbonates. Copolymer of DTE carbonate and 5% PEG and DTO carbonate have the lowest cell number in both the control and induction groups. Cell number in the control media for each polymer generally was higher than in the

induction media. Cells grown in the induction media on all polymers had similar cell number although the least number of cells still was present on DTE – 5% PEG carbonate.

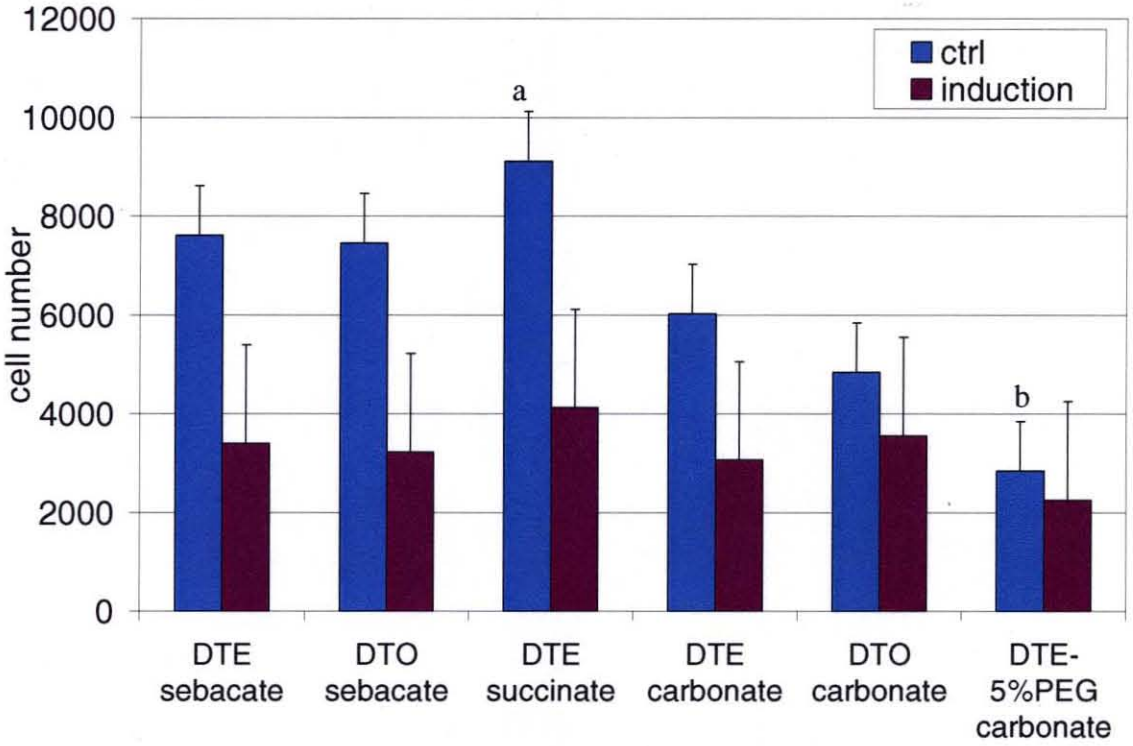

Figure 4.7 Cell numbers in control and induction group on various polymer surface at day 4. a: Highest cell number on DTE succinate in control group ($p<0.05$). b: Lowest cell number on DTE carbonate-5% PEG in control group ($p<0.05$).

4.3 Cell Morphology and Characterization

24 hours after adding the induction media, some cells had morphology resembling neuron-like cells indicated by arrow head and pre-mature neuron cells indicated by the arrow in Figures 4.8-4-10. The neuron-like morphology appeared in all induction groups for all polymer surfaces (Figures 4.8 and 4.9) and appeared to be very similar to the neuron-like morphology in the tissue culture plastic group (Figure 4.10).

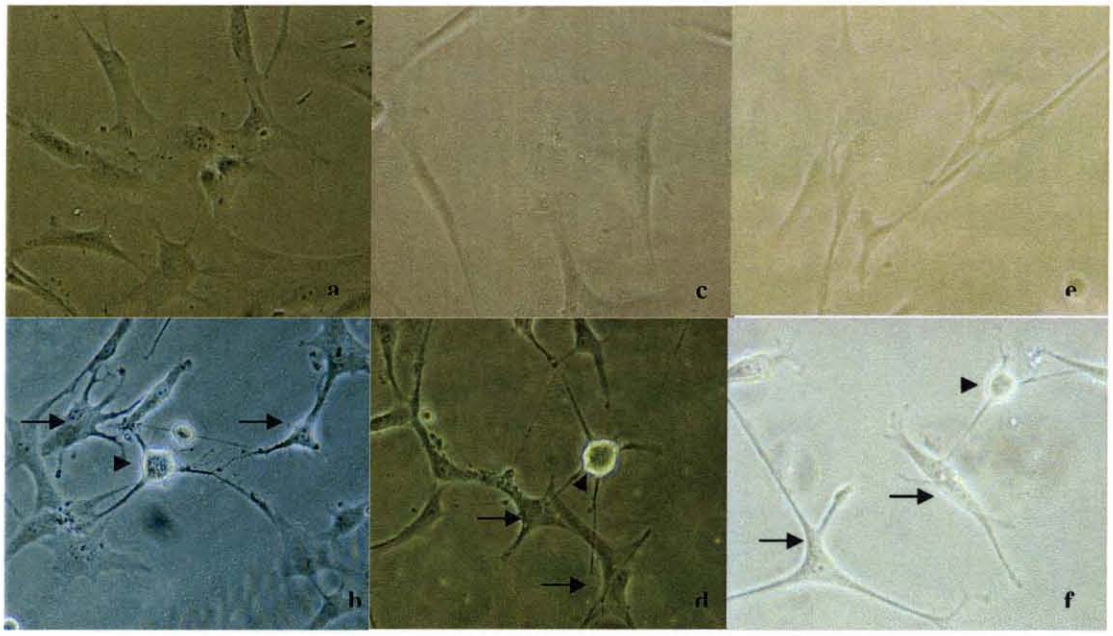

Figure 4.8 Morphology of induced MSC on polycarbonate polymer surfaces at 24 hours after induction (x40). Top row: control group. Bottom row: Induction group. From left column to right: poly DTE carbonate, poly DTO carbonate, poly DTE – 5% PEG carbonate. Arrow head indicates neuron-like morphology. Arrow indicates immature neuron-like morphology.

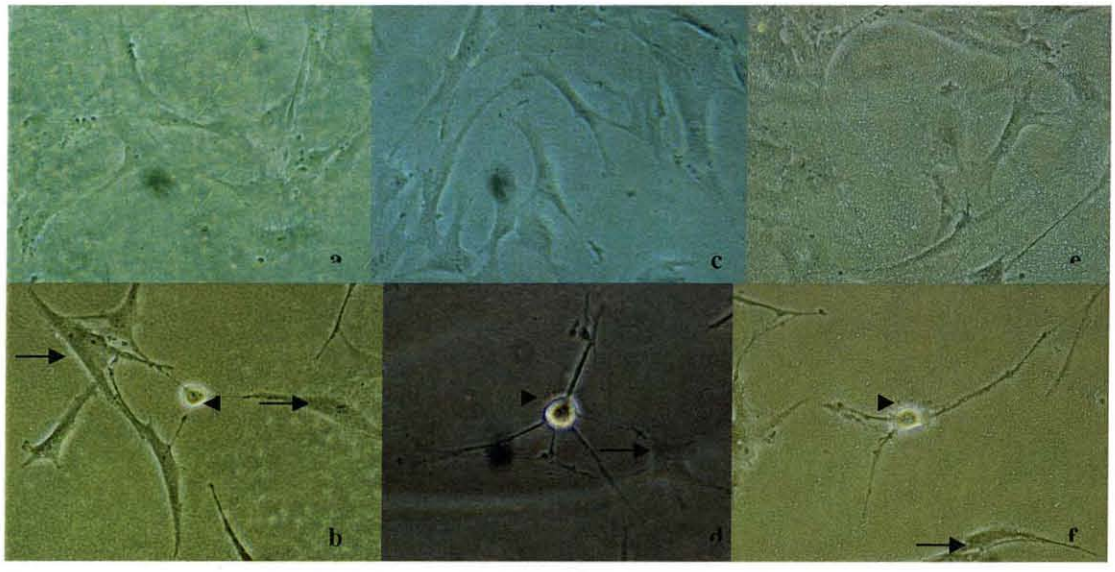

Figure 4.9 Morphology of induced MSC on polyarylate polymer surfaces at 24 hours after induction (x40). Top row: control group. Bottom row: Induction group. From left column to right: poly DTE sebacate, poly DTO sebacate, poly DTE succinate. Arrow head indicates neuron-like morphology. Arrow indicates immature neuron-like morphology.

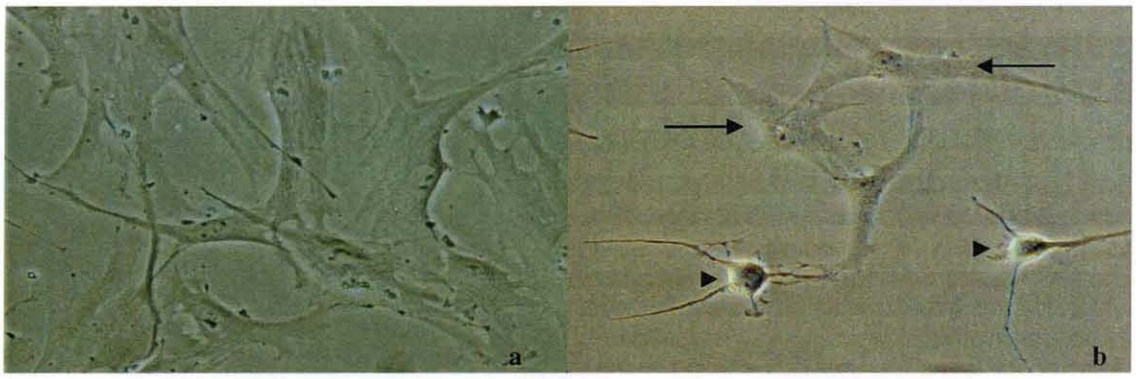

Figure 4.10 Morphology of induced MSC on tissue culture plastic at 24 hours after induction (x40). Left: control group. Right: Induction group. Arrow head indicates neuron-like morphology. Arrow indicates immature neuron-like morphology.

The neuron-like morphology was characterized by the bright glowing-round nucleus. On polymer surfaces, dead cells may resemble the bright glowing nucleus. The best way to distinguish a dead cell and a nucleus was by associating with neurite extension. As appeared in Figure 4.8-4.10, all neuron-like cells showed some sort of

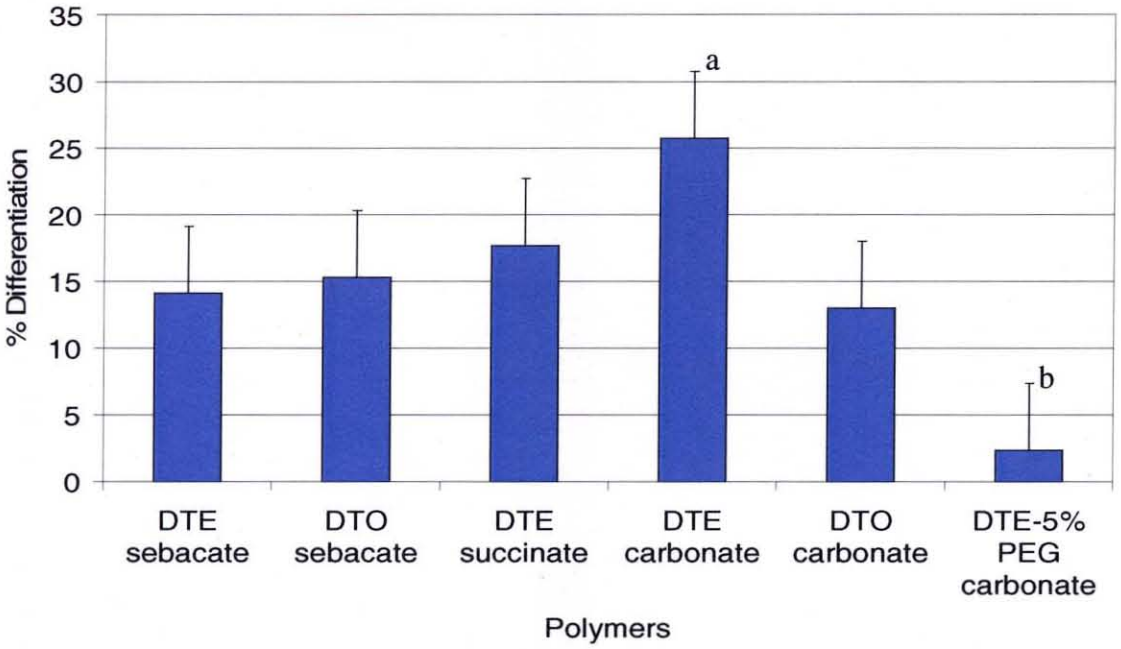

Figure 4.11 Percentage of neural differentiation of MSC on various polymer surfaces. a: poly DTE carbonate has the highest differentiation percentage ($p<0.05$). b: poly DTE carbonate – 5% PEG has the lowest percentage of differentiation ($p<0.05$).

extension from the bright nucleus which dead cells would lack. The immature neuron-like morphology was not as spread out as the normal MSC. It usually became more concentrated into one area and prepared to form the round nucleus. MSC growing on poly DTE carbonate (Figure 4.8a) and poly DTE sebacate (Figure 4.9a) had a flat and spread out morphology similar to MSC growing on tissue culture plastic (Figure 4.8a) in the control group. MSC seemed to be least spread out on poly DTE carbonate – 5% PEG surface (Figure 4.8e).

The percentage of neural differentiation was calculated by counting neuron-like cells in random fields (x20) (Figure 4.11). Poly DTE carbonate depicted the highest percentage of differentiation and copolymer of poly DTE carbonate and PEG had the lowest percentage of neural differentiation. The differences among the polyarylate polymers used were not as large as the ones among the polycarbonate polymers used. However, cells on DTE succinate demonstrated a slightly higher percentage of differentiated cells as compare to other polyarylate surfaces.

The neuron marker used was the neuron-specific enolase (NSE) which targeted specific protein on the nucleus. The NSE seemed to be also staining the immature neurons as shown in Figure 4.11. Cells were also stained with Fluorescein-Phalloidin which targets the actin filaments of the cell cytoskeleton. Induced MSC expressed NSE on all polymer surfaces (Figures 4.12 and 4.13). The NSE only stained the nucleus of the neuron-like cells. The neurite extension was stained by the Fluorescein-Phalloidin stain. The combination image clearly maps out the nucleus and neurite extension on all polymer surfaces. Cell on poly DTE carbonate – 5% PEG did not extend as many and as

long as compared to other polymer surfaces (Figure 4.12). MSC growing on tissue culture plastic in the induction group showed similar results (Figure 4.14).

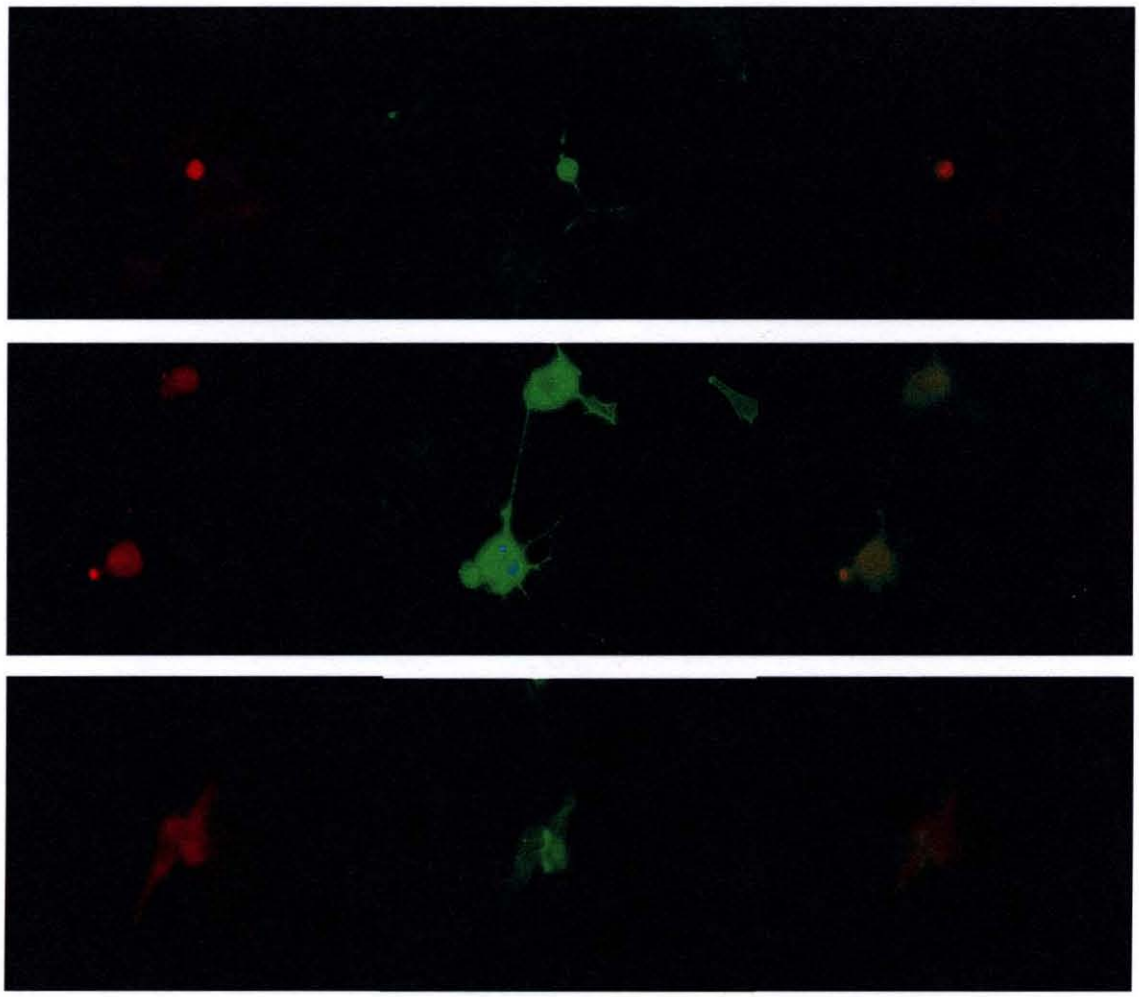

Figure 4.12 Fluorescent images of induced mesenchymal stem cell at 24 hours after induction (x40). Left: NSE stain. Middle: Fluorescein-Phalloidin stain. Right: Combined image of NSE and Fluorescein-Phalloidin stain. From top to bottom: poly DTE carbonate, poly DTO carbonate, poly DTE carbonate - 5% PEG.

The Fluorescein-Phalloidin stain of the control group on various polymer also showed the MSC growing on poly DTE carbonate, sebacate, and succinate were more spread out (Figures 4.15a, 4.15b, 4.15f) than on the poly DTE carbonate – 5% PEG, poly

DTO carbonate and sebacate (Figures 4.15c, 4.15d, 4,15e). The cytoskeleton seemed to be organized randomly on all polymer surfaces.

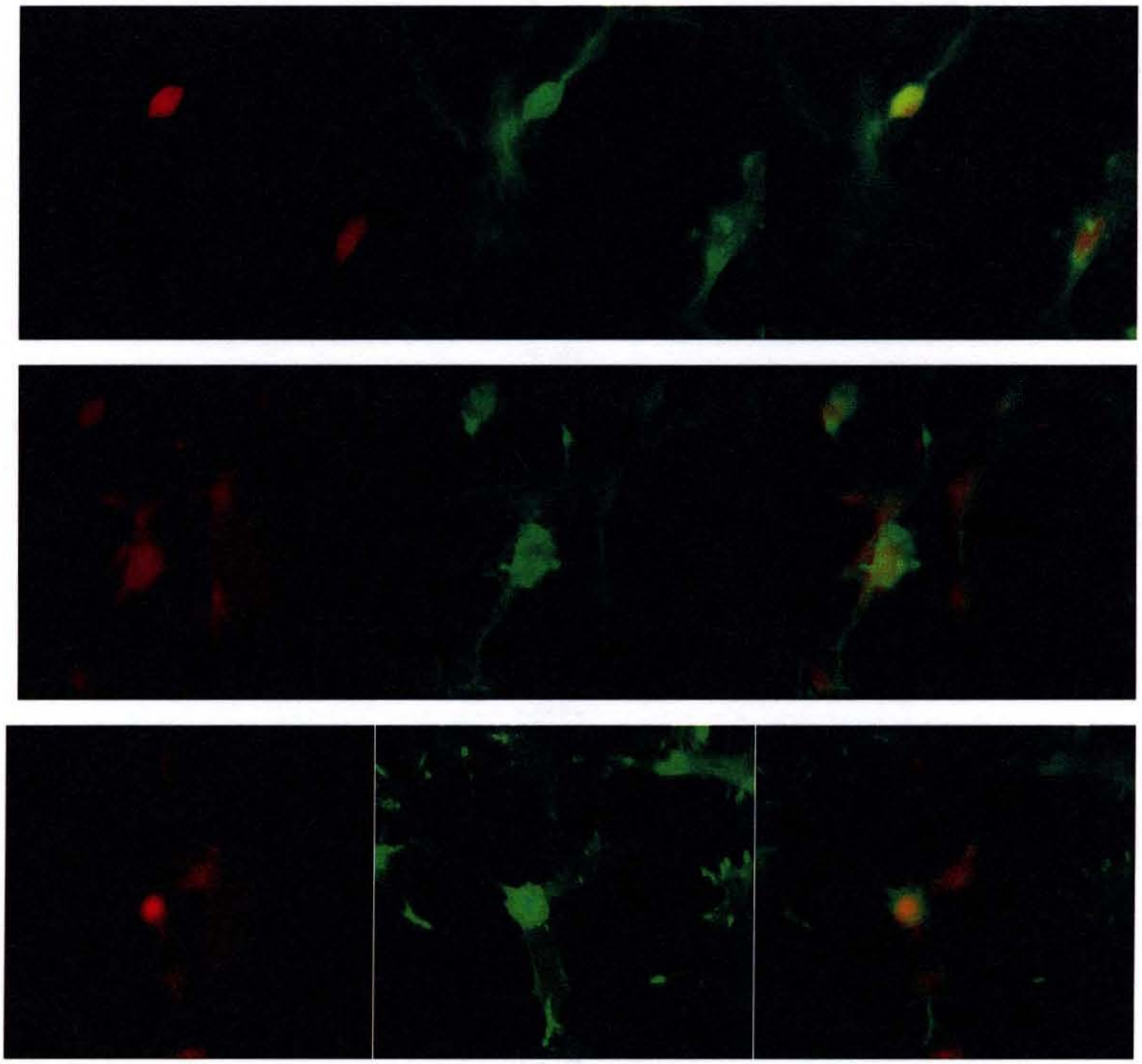

Figure 4.13 Fluorescent images of induced mesenchymal stem cell at 24 hours after induction (x40). Left: NSE stain. Middle: Fluorescein-Phalloidin stain. Right: Combined image of NSE and Fluorescein-Phalloidin stain. From top to bottom: poly DTE sebacate, poly DTO sebacate, poly DTE succinate.

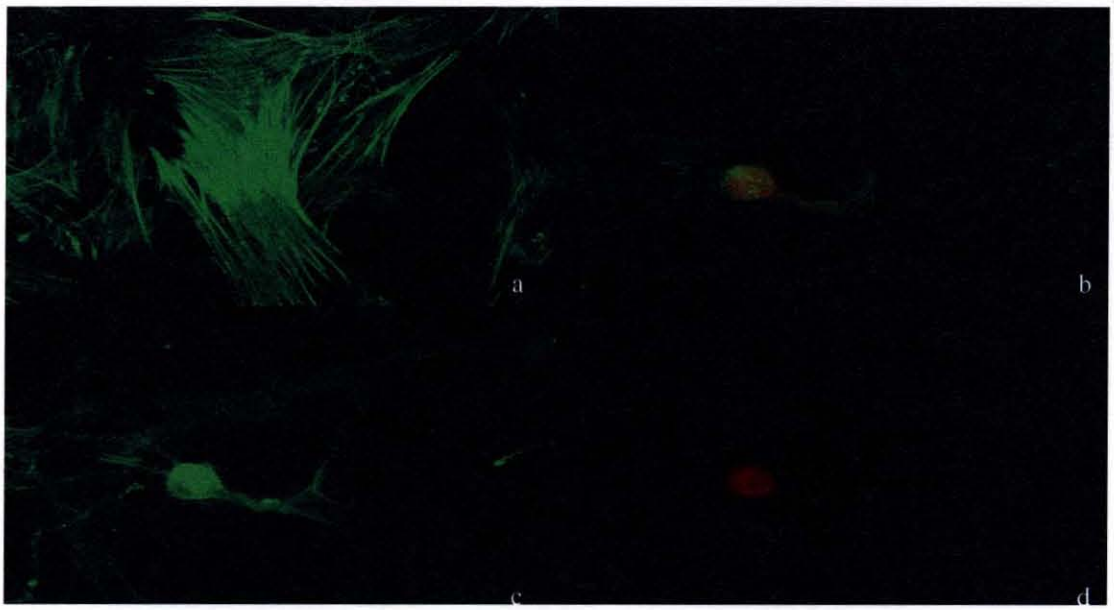

Figure 4.14 a: Fluorescein-Phalloidin fluorescent images of MSC in the control group at 24 hours after induction (x40). Fluorescent images of induced MSC at 24 hours after induction (x40). b: Combined image of NSE and Fluorescein-Phalloidin. c: NSE stain. d: Fluorescein-Phalloidin stain.

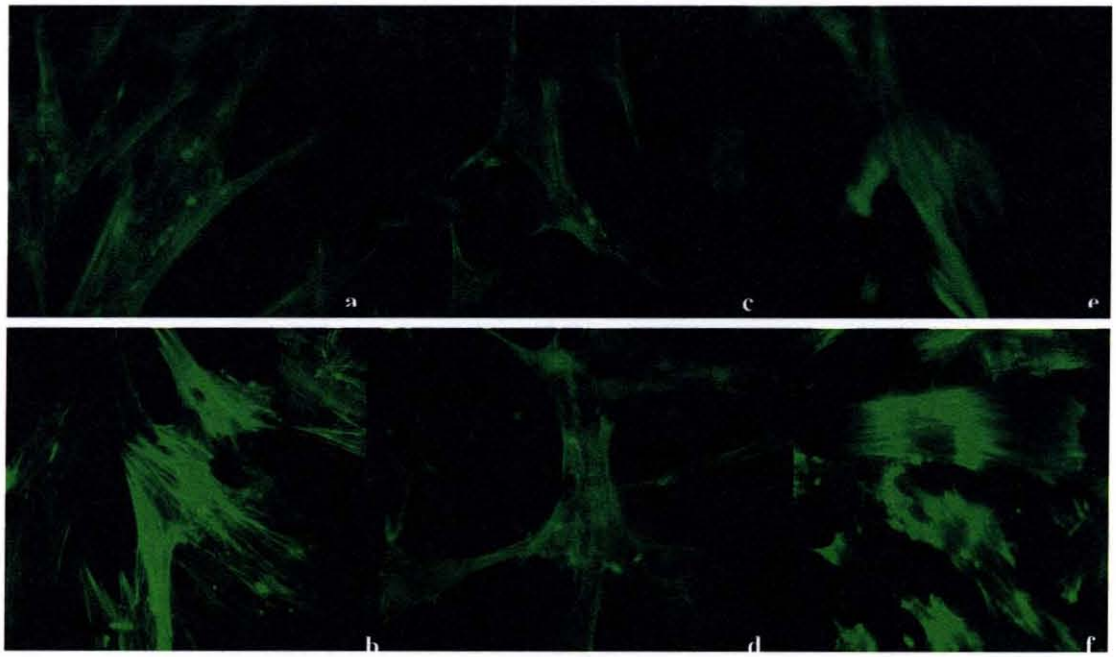

Figure 4.15 Fluorescein-Phalloidin fluorescent images of MSC in the control group at 24 hours after induction (x40) on various polymer surfaces. Top row from left to right: poly DTE carbonate, poly DTO carbonate, poly DTE carbonate – 5% PEG. Bottom row from left to right: poly DTE sebacate, poly DTO sebacate, poly DTE succinate.

CHAPTER 5

CONCLUSION AND SUGGESTION FOR FUTURE RESEARCH

The advantage of using polymers for scaffold fabrication is the feasibility of processing and manipulation. The polymer in this study is soluble in many organic solvent thus providing a larger spectrum of fabrication processes. However, one important issue in polymer processing is solvent residue. The properties and performance of the scaffold will be affected if solvents are still present. The casting method used has shown that very little solvent remained in the polymer films, hence suggesting its future use for scaffold fabrication.

All polymers showed high thermal stability with 10% weight loss temperatures above 300°C (Appendix A). Increase in pendent chain length of polycarbonates has decreased the T_g and increased the wettability as previously described [28]. Low glass transition temperatures (T_g) (Appendix B), high decomposition temperature and lack of crystallinity allow polycarbonate polymers to be processed in various thermal processing techniques. Increase in PEG content has decreased the T_g and has a higher water contact angle. The endothermic process upon heating and exothermic event upon cooling of polyarylates showed similar behavior to previous study [57]. The T_g of the polyarylates, DTO sebacate, was below body temperature, hence the polymers will assume to be in a rubbery state if used in vivo and may explain findings in this study with regards to maintaining cell growth and differentiation that was characterized as being hydrophobic. Either increasing in the pendent chain or the backbone will decrease the T_g where T_g of DTE succinate was the highest followed by DTE sebacate and DTO sebacate as expected

[29]. The water contact angle was more dependent on the pendent chain for the polyarylates as previously described [29].

Cell spreading and growth are influenced significantly by the surface properties such as the wettability, charge, rigidity, and surface structure in the polymer-cell interaction [23,53,58-62]. Cell proliferation on oxygen-containing diacid backbone polymers is independent of the water contact angle [64]. MSC growth was uniformly well on the polyarylate substrates. DTE succinate had the highest cell number and may be due to the combination effect of its short diacid backbone and pendent chain. Cell proliferation on backbone polymers such as polycarbonates is significantly dependent on the wettability of the surface [28,64] and exhibited high linear correlation between cell number and wettability (Figure 4.6). The wettability was more linearly correlated to the percentage of neural differentiation. It suggested the most hydrophobic polycarbonates are a less stimulating substrate for MSC proliferation and neural differentiation. Recent studies have demonstrated that the osteogenic differentiation of MSC was enhanced on the more hydrophobic polyarylates surfaces [32,33]. However, this trend was not clearly seen in this study (Figure 4.11).

Poly DTE carbonate was the least hydrophobic substrate and stimulated MSC proliferation and differentiation. However, the copolymer of poly DTE carbonate and 5% PEG was a more hydrophobic surface and had poor MSC proliferation and differentiation similar to previous finding [30]. Increase in PEG content in the copolymers will significantly reduce the cell proliferation and at 5% PEG content, the cells tend to aggregate rather than spreading out [67] In this study, MSC depicts similar behavior on the copolymer with 5% PEG. These cells were able to be removed easily

after gentle wash. The spreading of the cell was influenced by the cohesion among the cells when overcoming the cell adhesion to the surface, the cells tends to aggregate.

This study has demonstrated the effect of substrate surface on MSC proliferation and differentiation. Cell-substrate interaction, cell orientation and spreading are important for directing cellular functions [23,53,66]. Various cellular behaviors are mediated by the binding affinity of integrins for ligands. Integrins are cellular surface receptor protein that recognize and bind to the amino regions of the ligands regulated by the ECM. The intergrin-ligand complex interacts with the cytoskeleton, thus coordinating cell migration, tissue organization, cell growth, inflammation, and differentiation [65]. Substrate protein adsorption is mediated via multiple electrostatic, hydrophobic, hydrogen bonding, and/or van der Waals interactions [66]. Protein adsorption will change the conformation or partial deform the protein when binding on to the substrate surface and is influenced by the surface properties of the substrates. The conformation changes are more traumatic on hydrophobic surfaces possibly resulting in poor cell proliferation [64] which is similar to the result of this study (Figure 4.7).

The differentiated neural-like cells had NSE expression and the nucleus of the immature neuron-like cells also was heavily stained with NSE. This suggested that NSE expression can be use to indicate early stage of MSC neural lineage differentiation. Other immunofluorescent can be used to identify for later stage i.e. synaptophysin, synaptic vehicle protein 2, tau, MAP2, and MAP3. Synaptophysin is the integral membrane protein in synaptic vesicles and synaptic vehicle protein 2 regulates the presynaptic calcium concentration during consecutive action potentials. MAP2, MAP 3, and tau are associated with the microtubule-associated proteins which promote oriented

polymerization and microtubules assembly. MAP2 is located in the dentrites and tau and MAP3 are located in the axon. Positive expression of the above indicators may also be functioning indicators. To reinsure the differentiated cells are functional, electrophysiology of these cells should be studied.

The advantage of inducing MSC with microenvironment factors is to reduce scaffold complexity. Reducing essential components for the tissue engineering design for neural repair may be beneficial for the host. Fabricating three-dimensional scaffolds with the tyrosine-derived polycarbonates and polyarylates may promote better differentiation. Further optimization of scaffold should involve investigating the polymer composition and geometric structure of the tyrosine-derived polycarbonates and polyarylates that will promote MSC proliferation and differentiation along the neural lineage.

APPENDIX A

TGA RESULTS

The TGA results for all polymers as received and after processed are included in this appendix. The DSC results showed (1) the complete cycle and (2) the partial of the cycle with temperature ranging from 50°C to 100°C for methylene chloride residue evaluation.

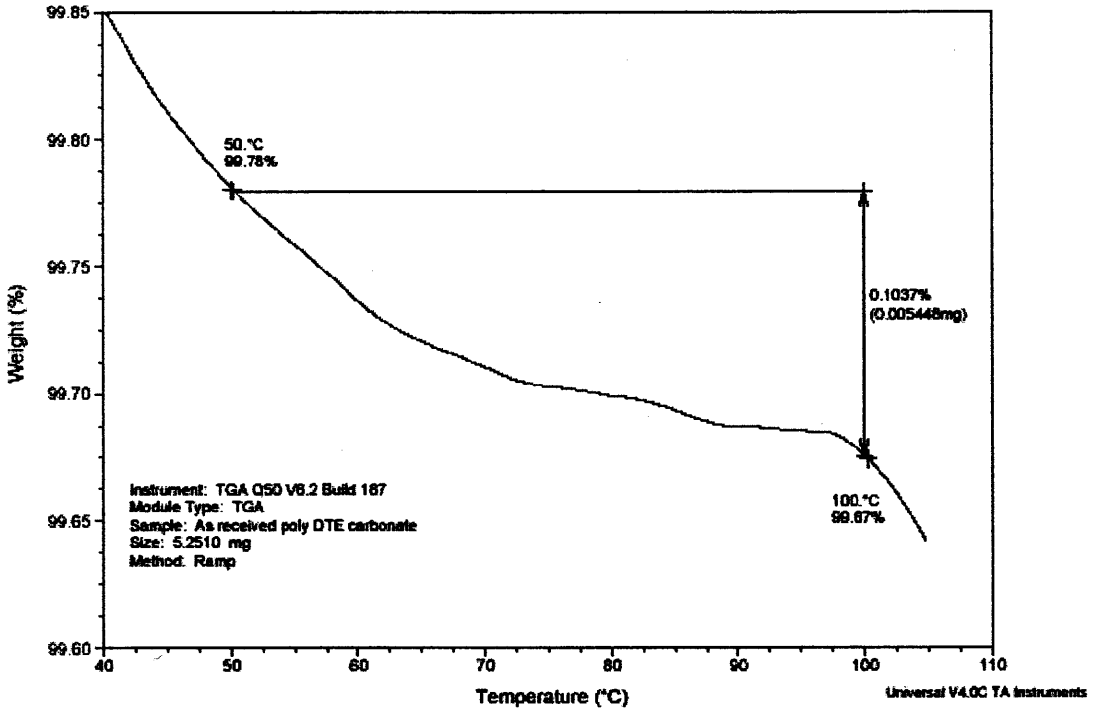

Figure A.1 TGA result in partial cycle of poly DTE carbonate in received form.

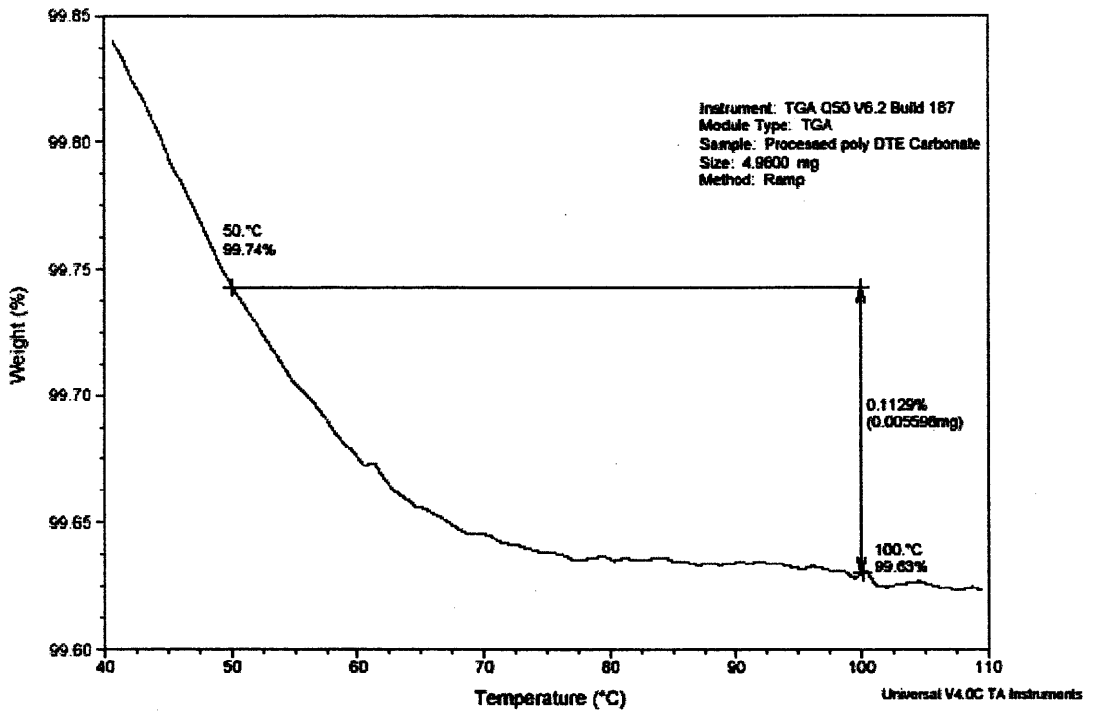

Figure A.2 TGA result in partial cycle of poly DTE carbonate in processed form.

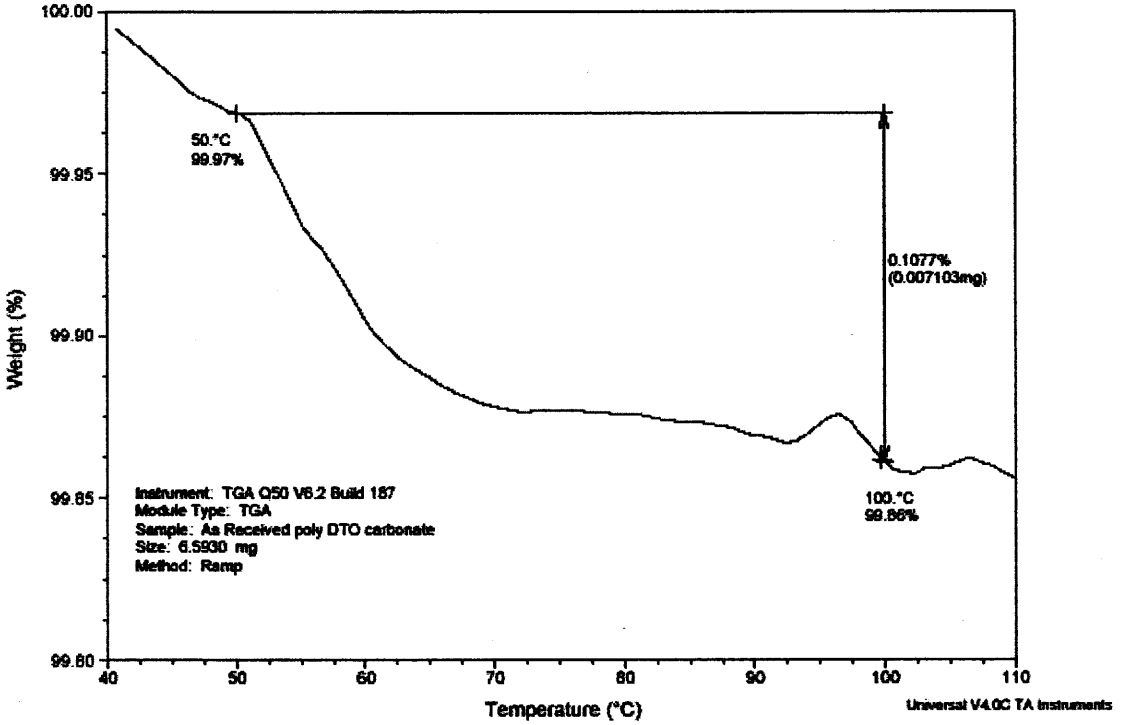

Figure A.3 TGA result in partial cycle of poly DTO carbonate in received form.

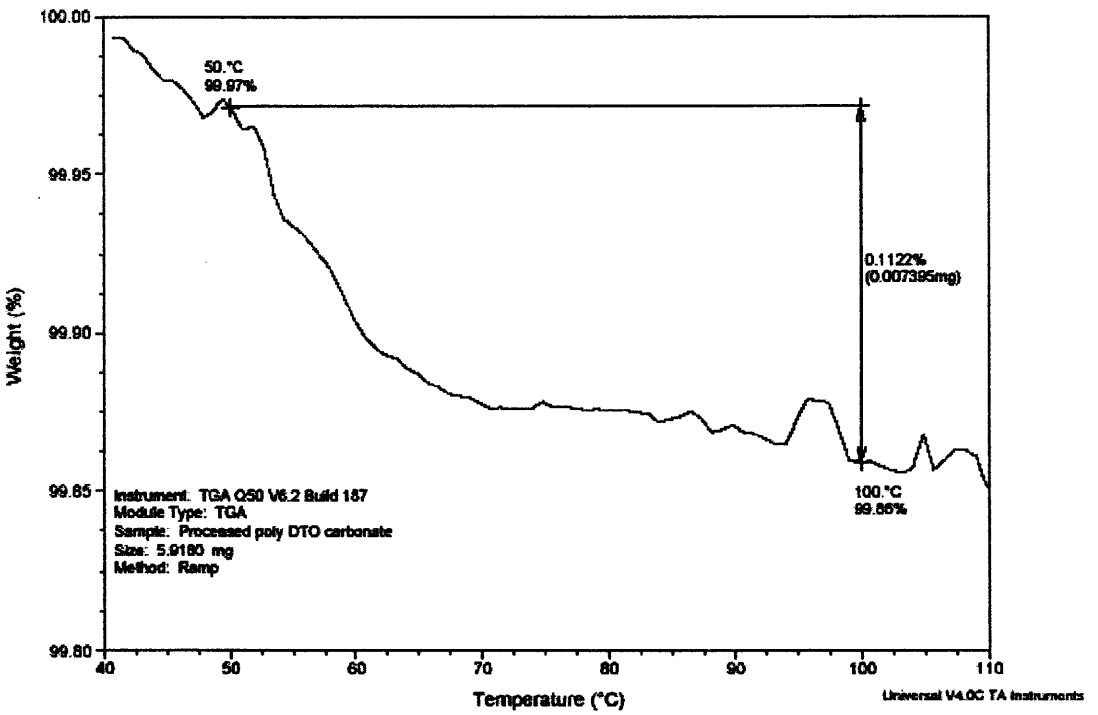

Figure A.4 TGA result in partial cycle of poly DTO carbonate in processed form.

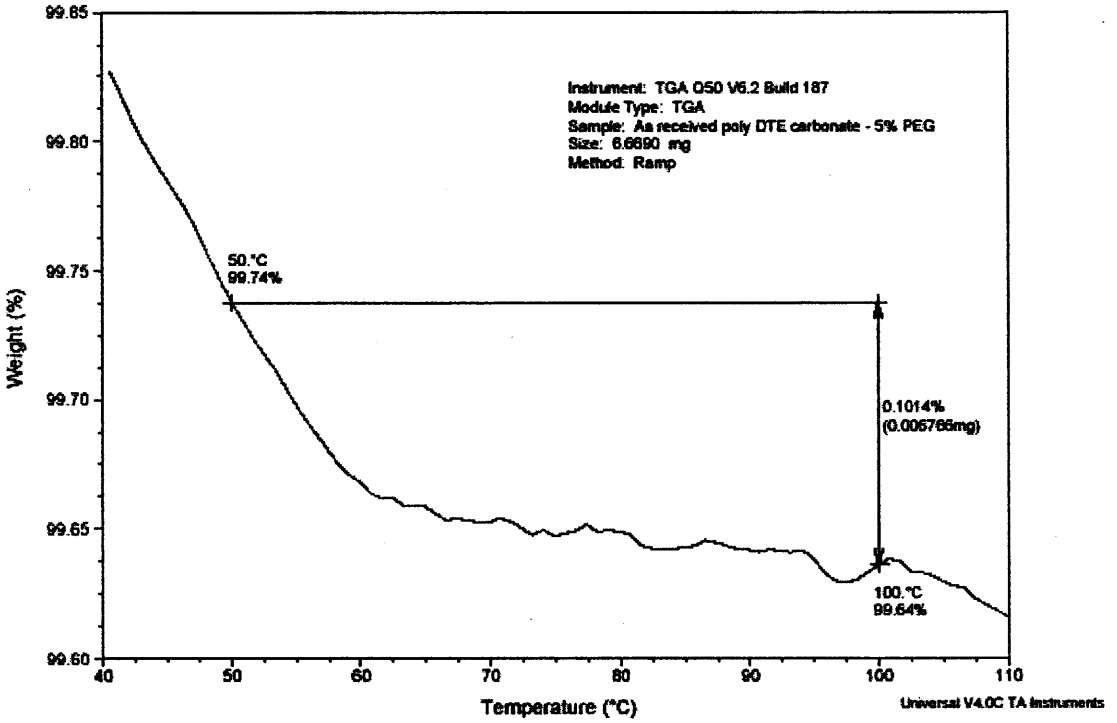

Figure A.5 TGA result in partial cycle of poly DTE carbonate – 5% PEG in received form.

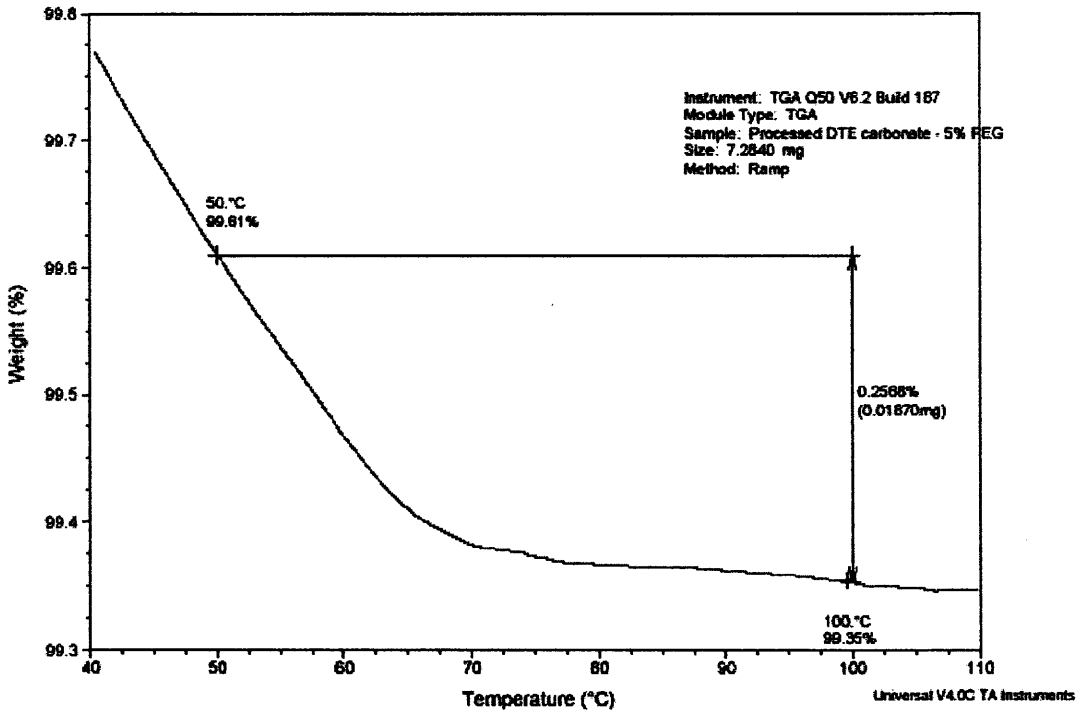

Figure A.6 TGA result in partial cycle of poly DTE carbonate - 5% PEG in processed form.

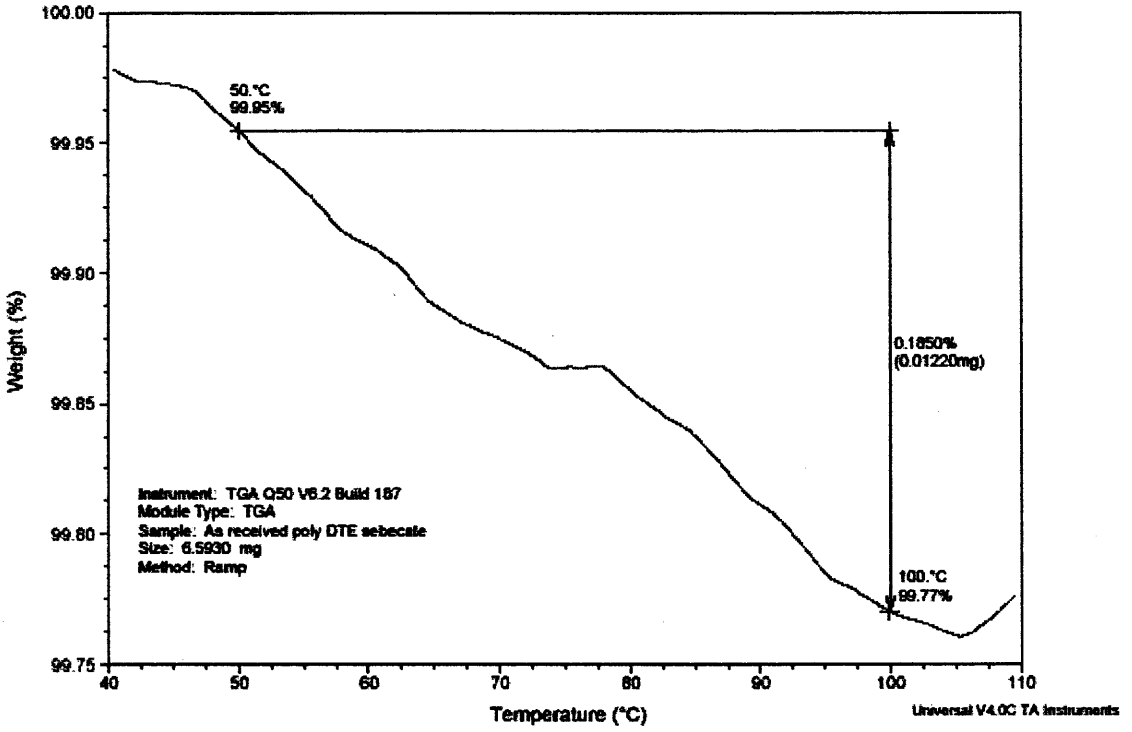

Figure A.7 TGA result in partial cycle of poly DTE sebecate in received form.

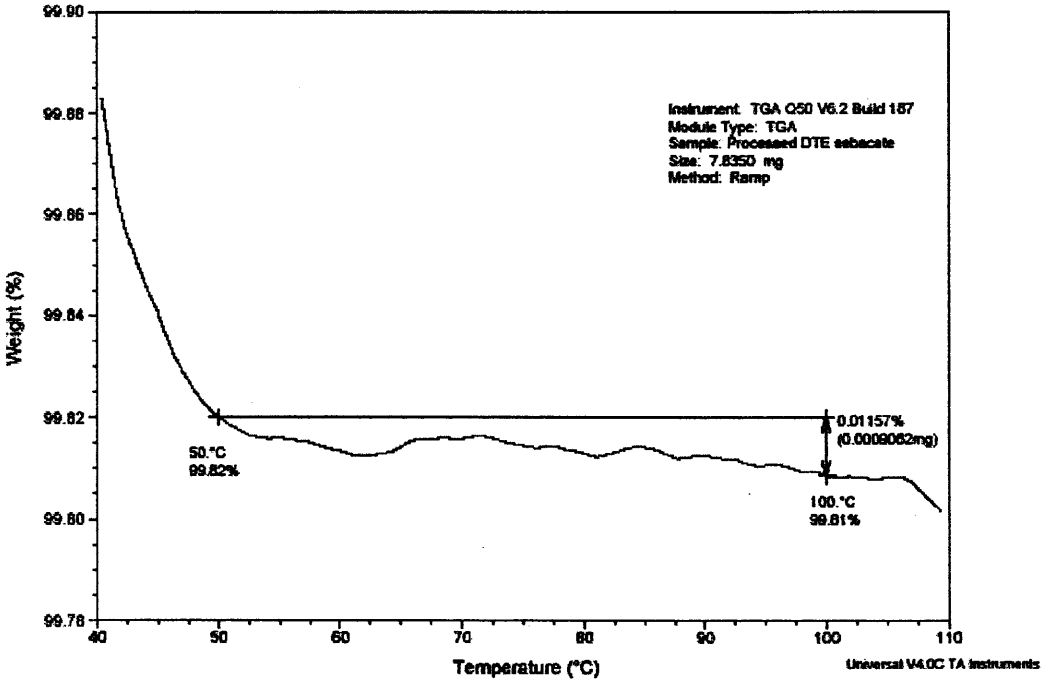

Figure A.8 TGA result in partial cycle of poly DTE sebecate in processed form.

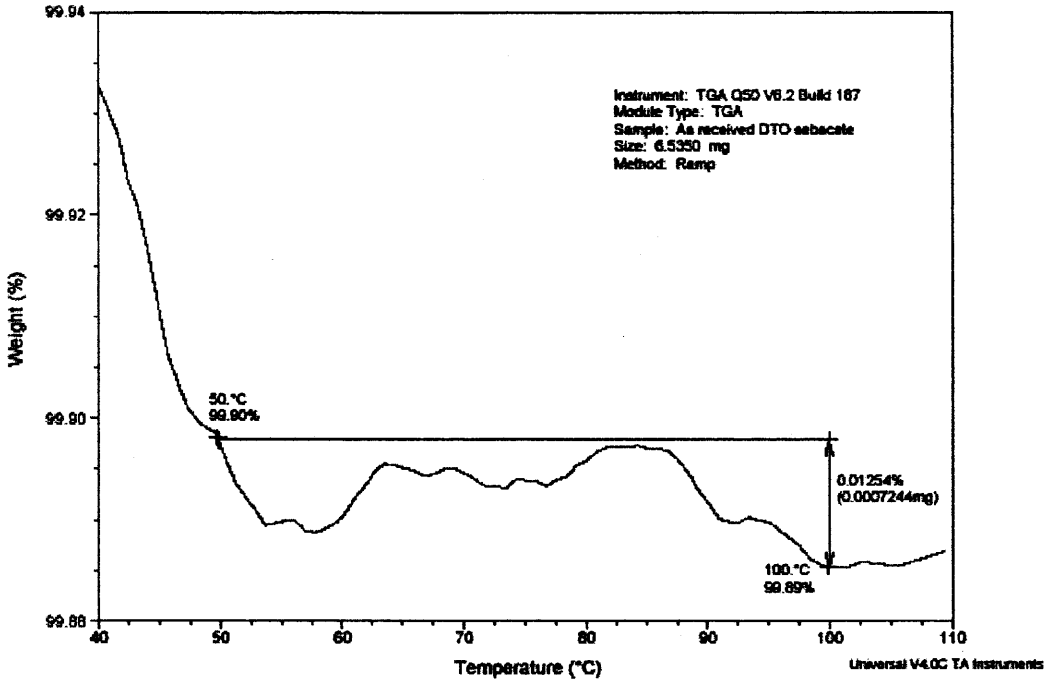

Figure A.9 TGA result in partial cycle of poly DTO sebecate in received form.

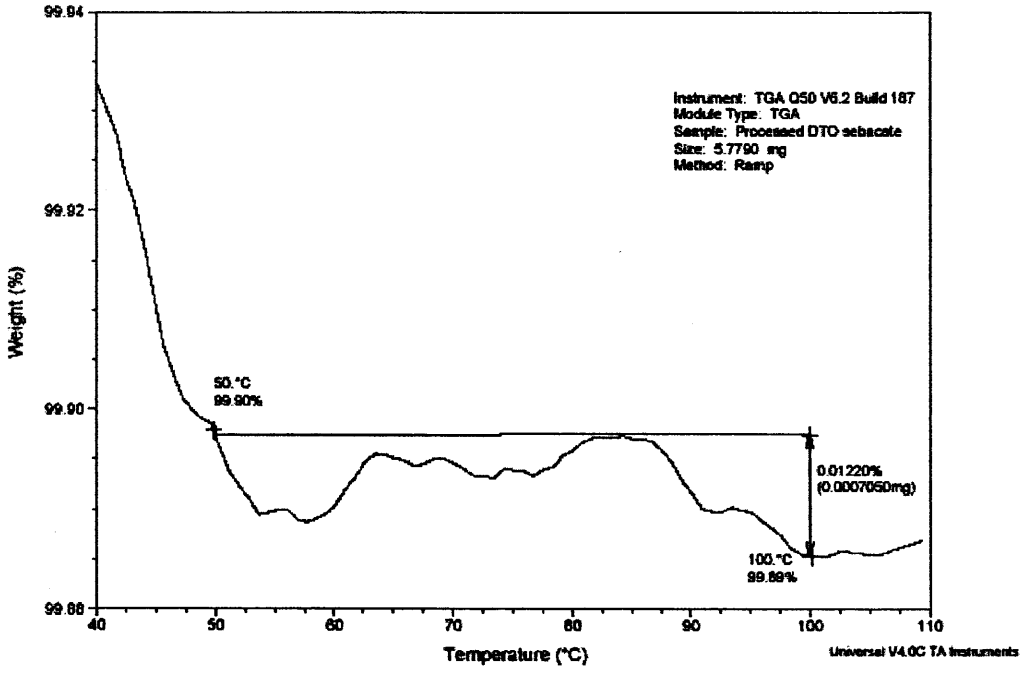

Figure A.10 TGA result in partial cycle of poly DTO sebecate in molded form.

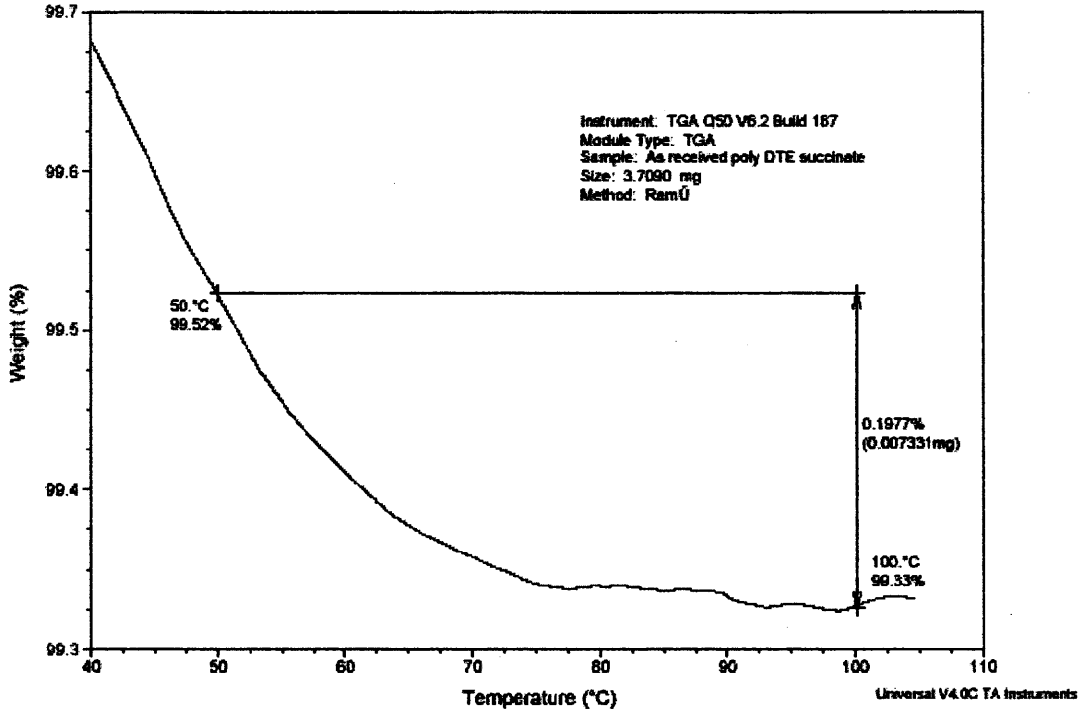

Figure A.11 TGA result in partial cycle of poly DTE succinate in received form.

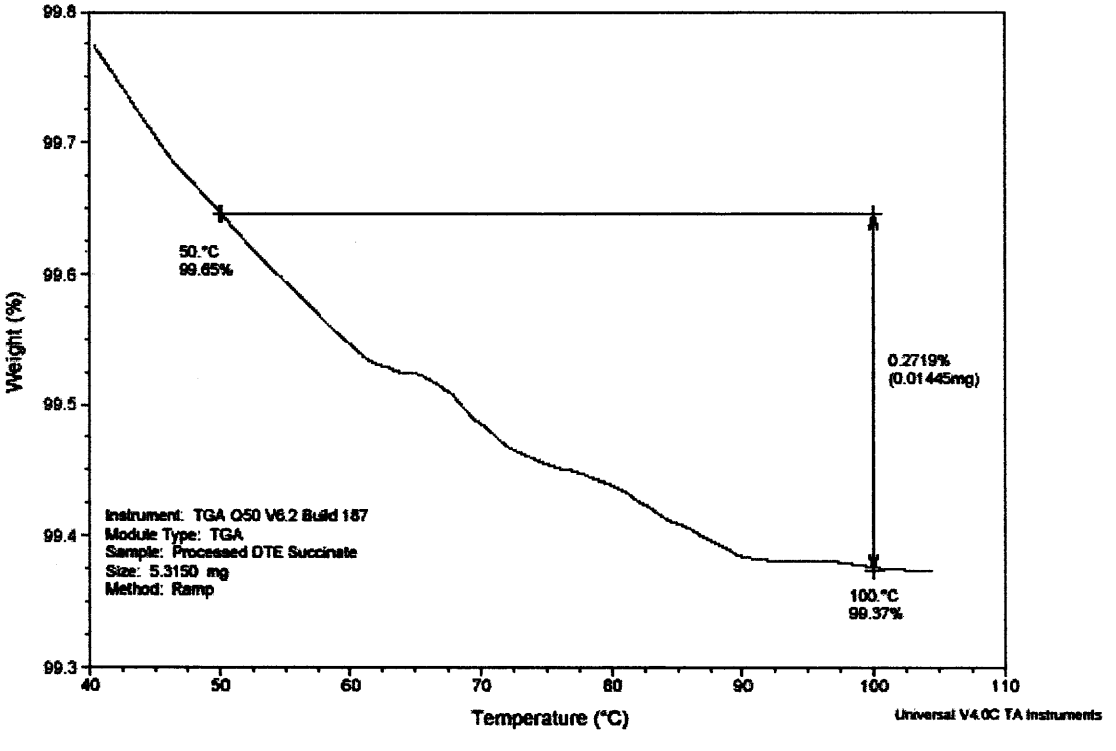

Figure A.12 TGA result in partial cycle of poly DTE succinate in processed form.

APPENDIX B

DSC RESULTS

The DSC results for all polymers as received and after processed are included in this appendix. The DSC results showed the complete cycle and transition temperature is determined.

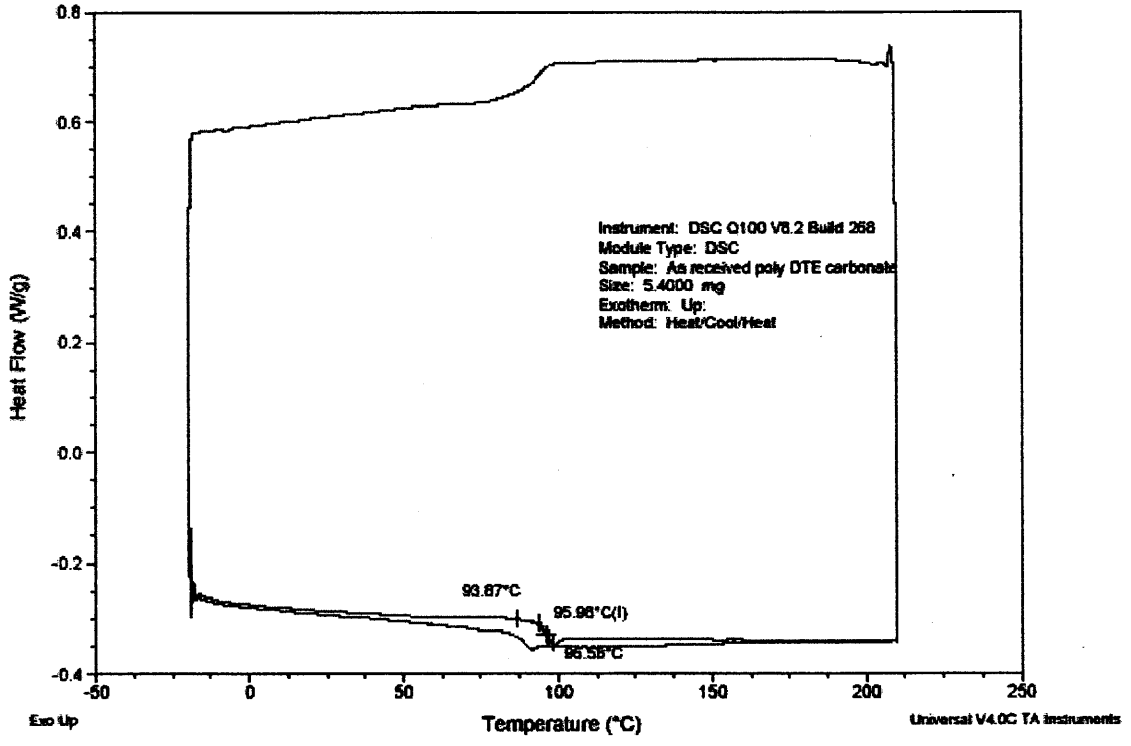

Figure B.1 DSC result of poly DTE carbonate in received form.

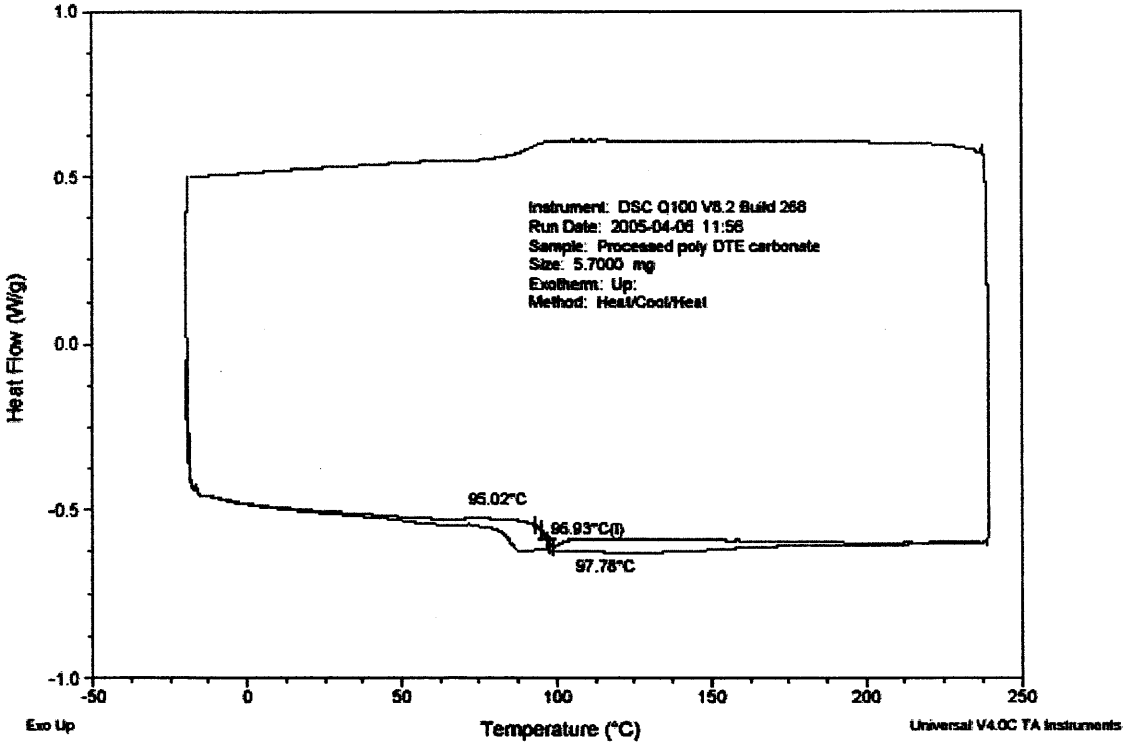

Figure B.2 DSC result of poly DTE carbonate in processed form.

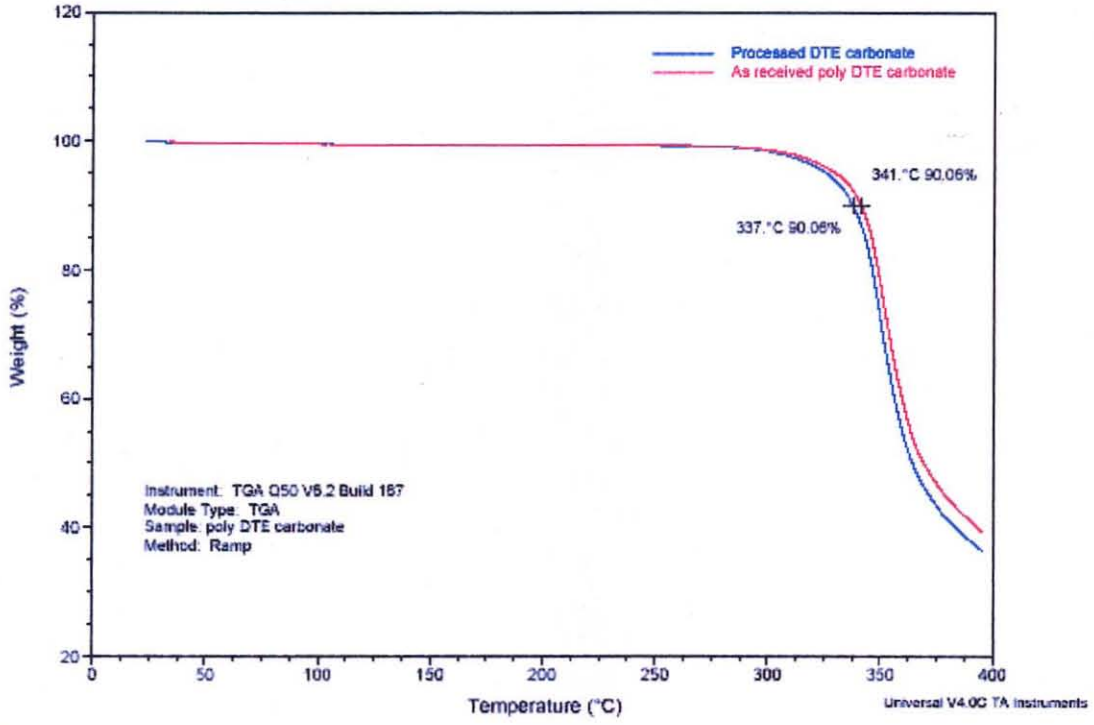

Figure A.13 TGA results in complete cycle of poly DTE carbonate in received and processed forms.

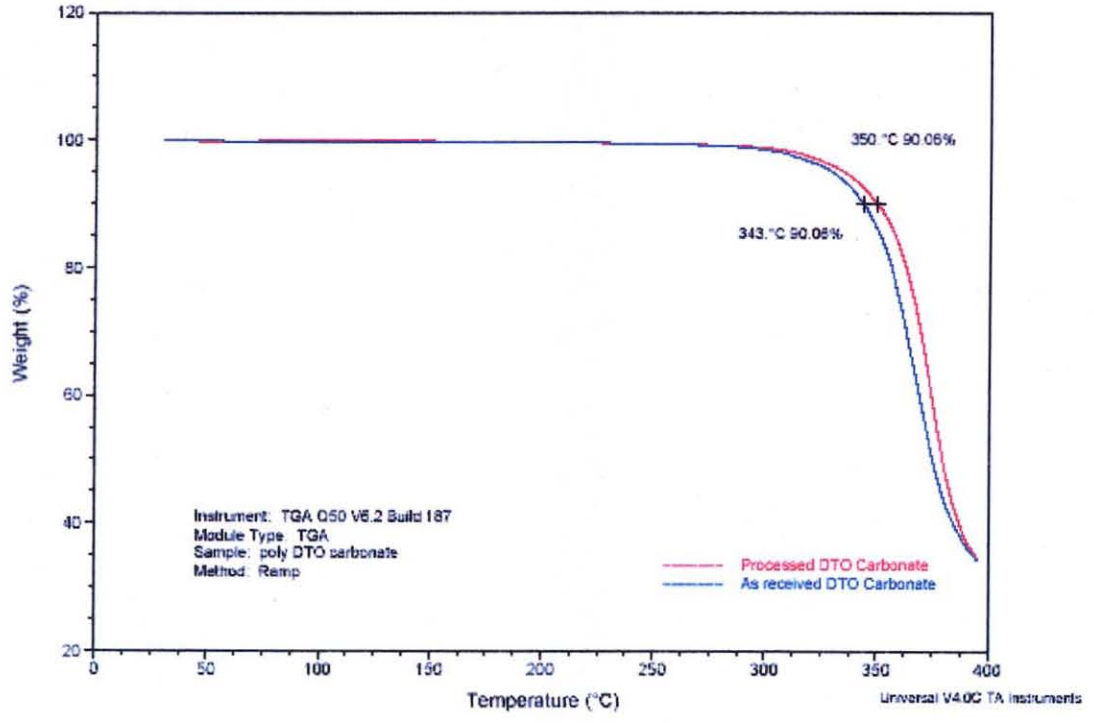

Figure A.14 TGA results in complete cycle of poly DTO carbonate in received and processed forms.

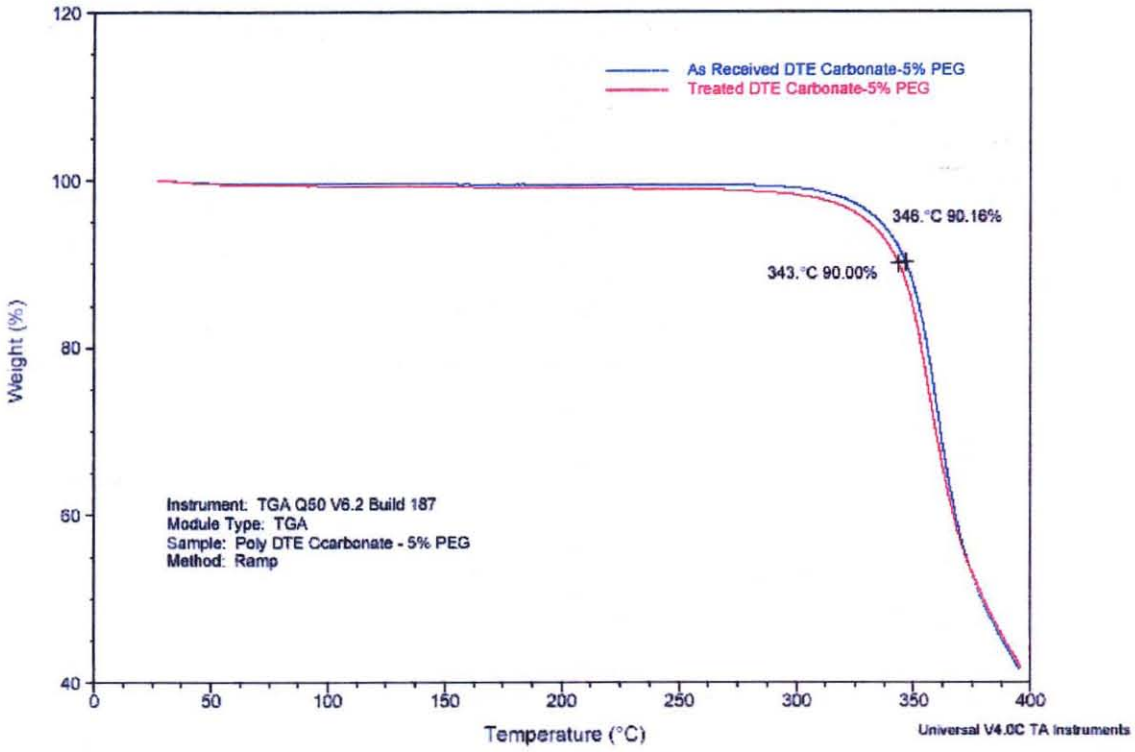

Figure A.15 TGA results in complete cycle of poly DTE carbonate – 5% PEG in received and processed forms.

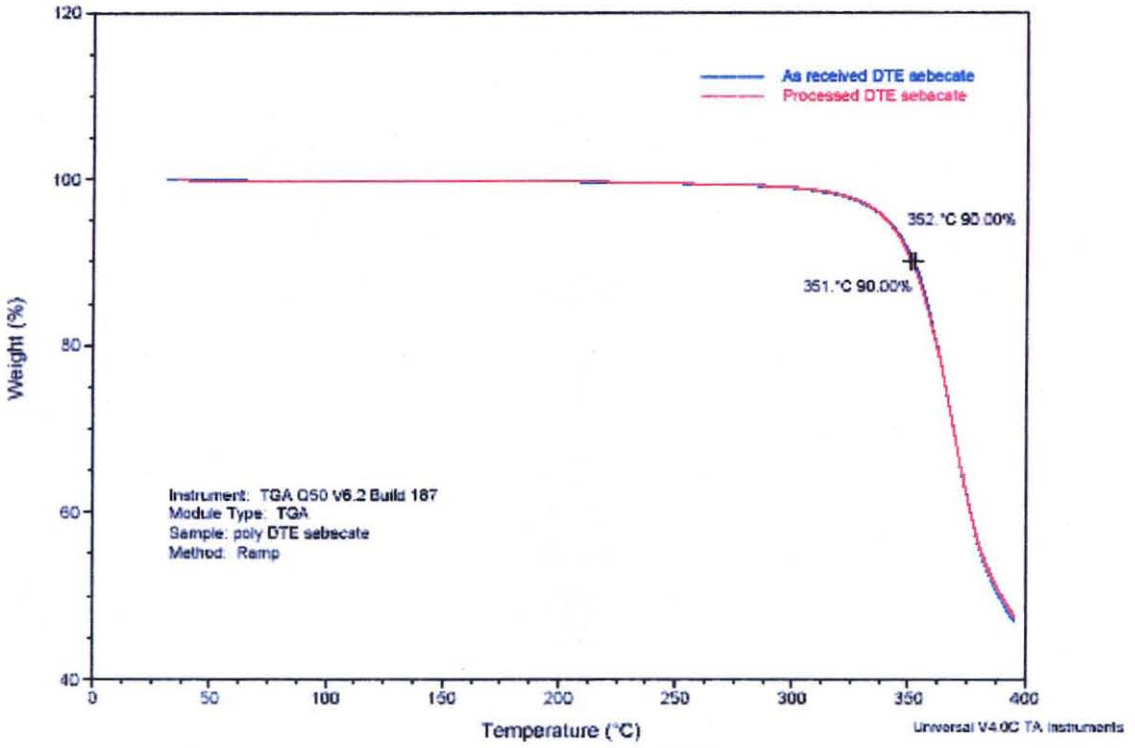

Figure A. 16 TGA results in complete cycle of poly DTE sebacate in received and processed forms.

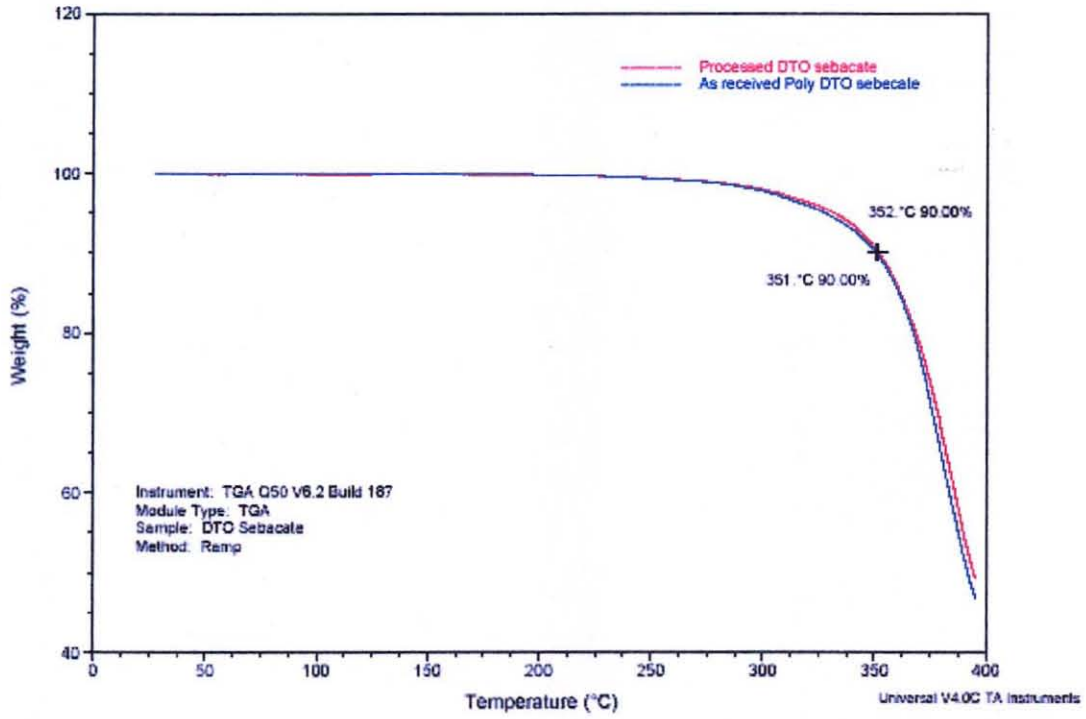

Figure A. 17 TGA results in complete cycle of poly DTO sebacate in received and processed forms.

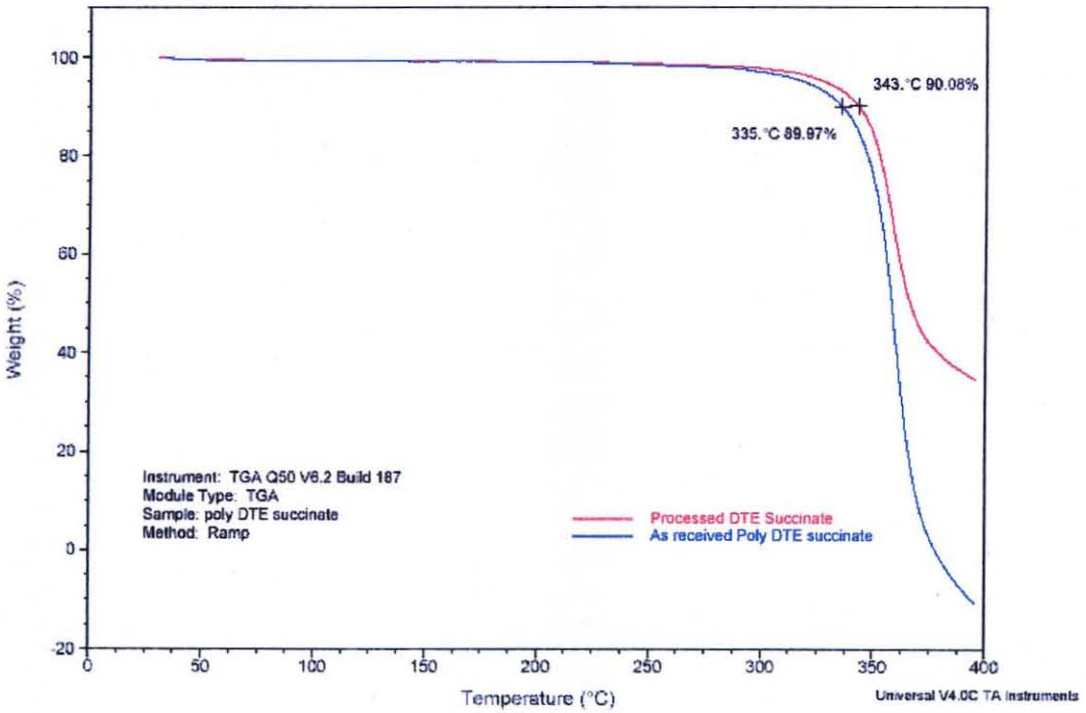

Figure A. 18 TGA results in complete cycle of poly DTO sebacate in received and processed forms.

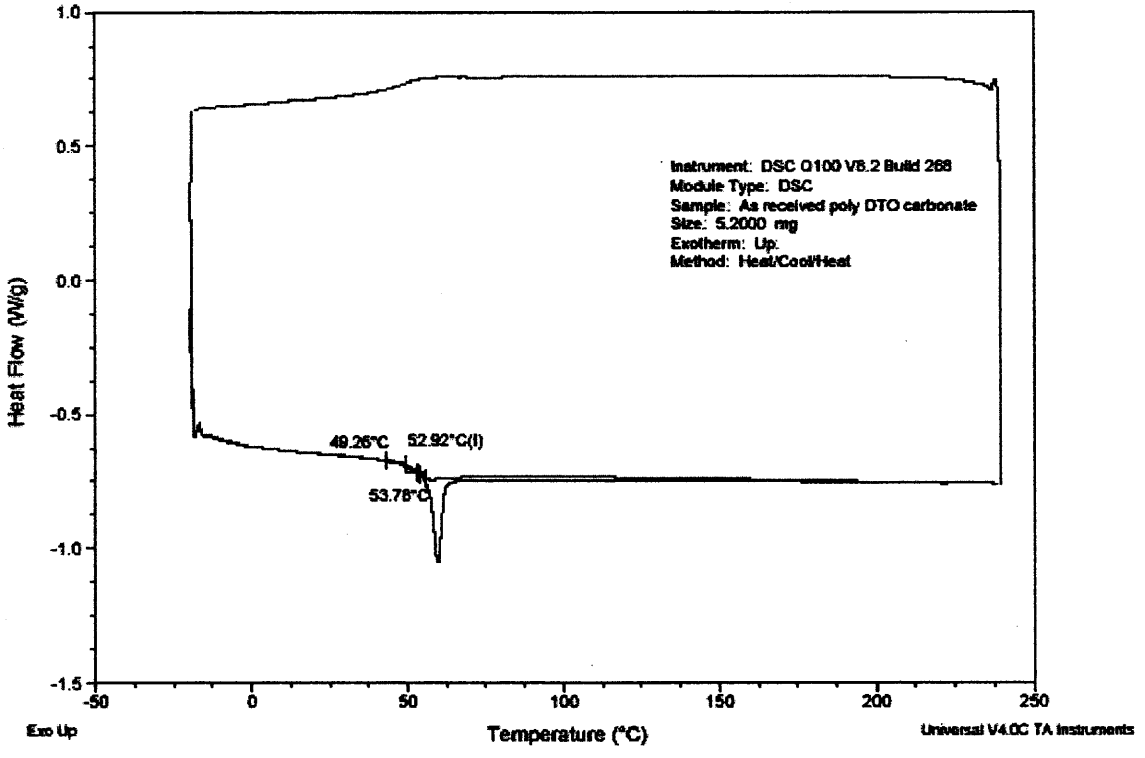

Figure B.3 DSC result of poly DTO carbonate in received form.

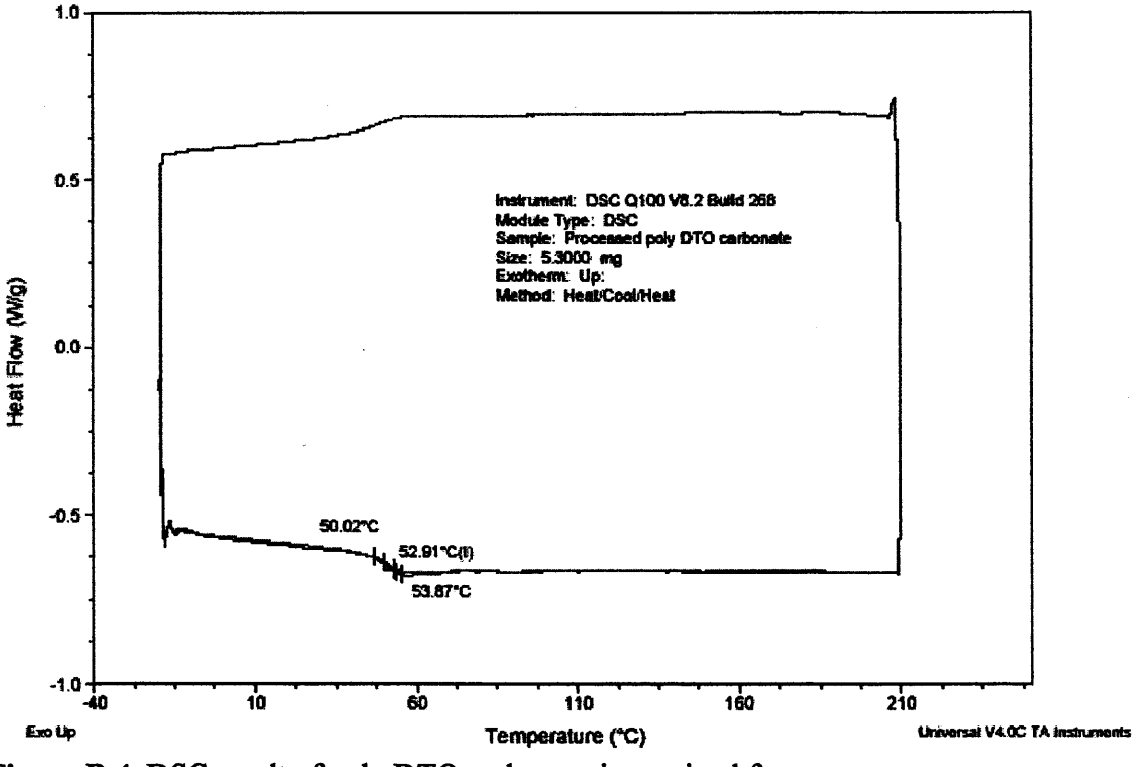

Figure B.4 DSC result of poly DTO carbonate in received form.

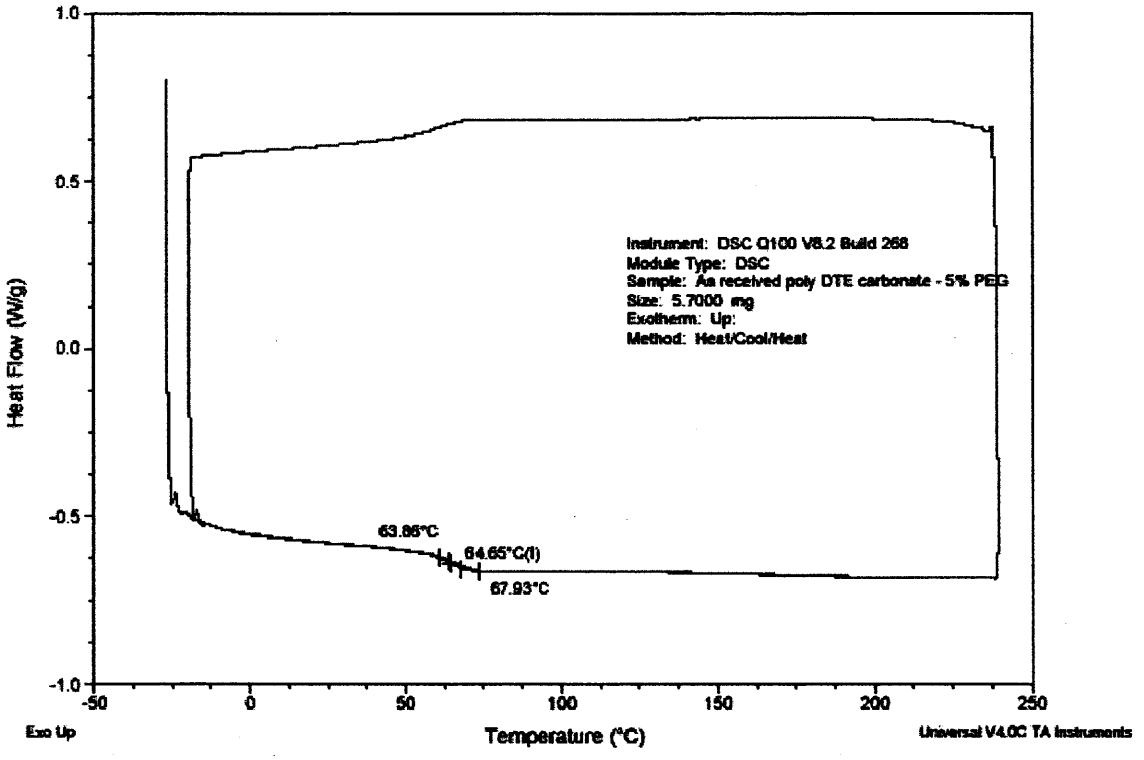

Figure B.5 DSC result of poly DTE carbonate-5% PEG in received form.

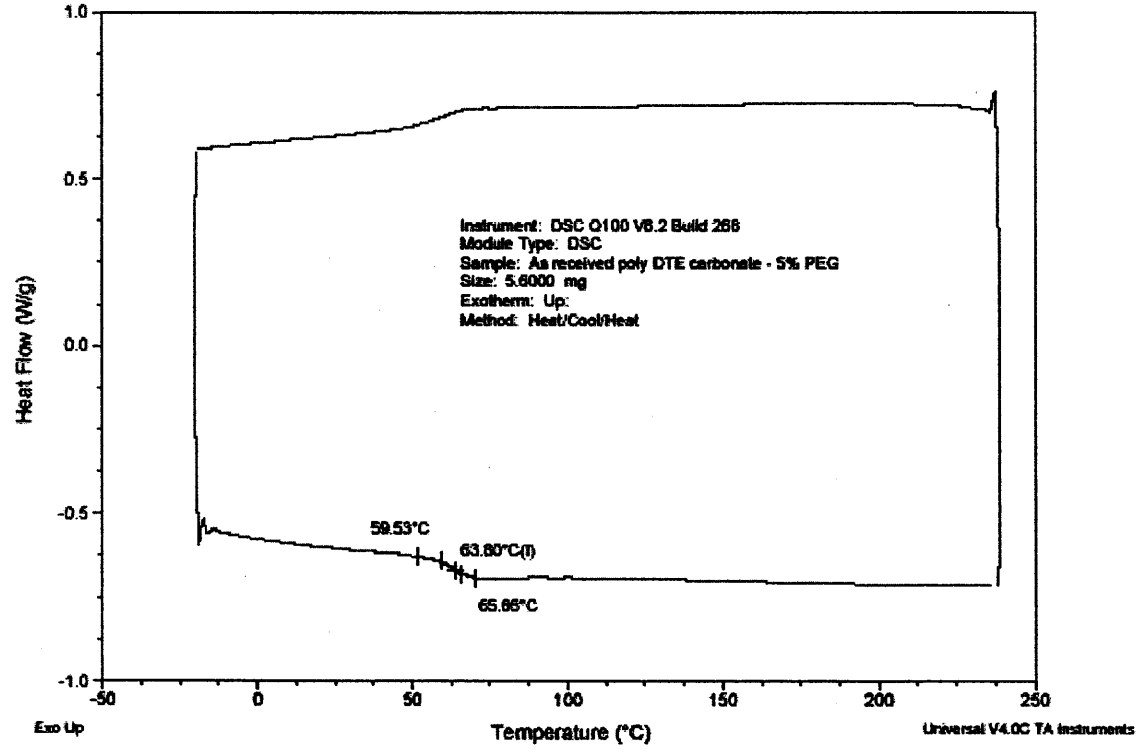

Figure B.6 DSC result of poly DTE carbonate-5% PEG in processed form.

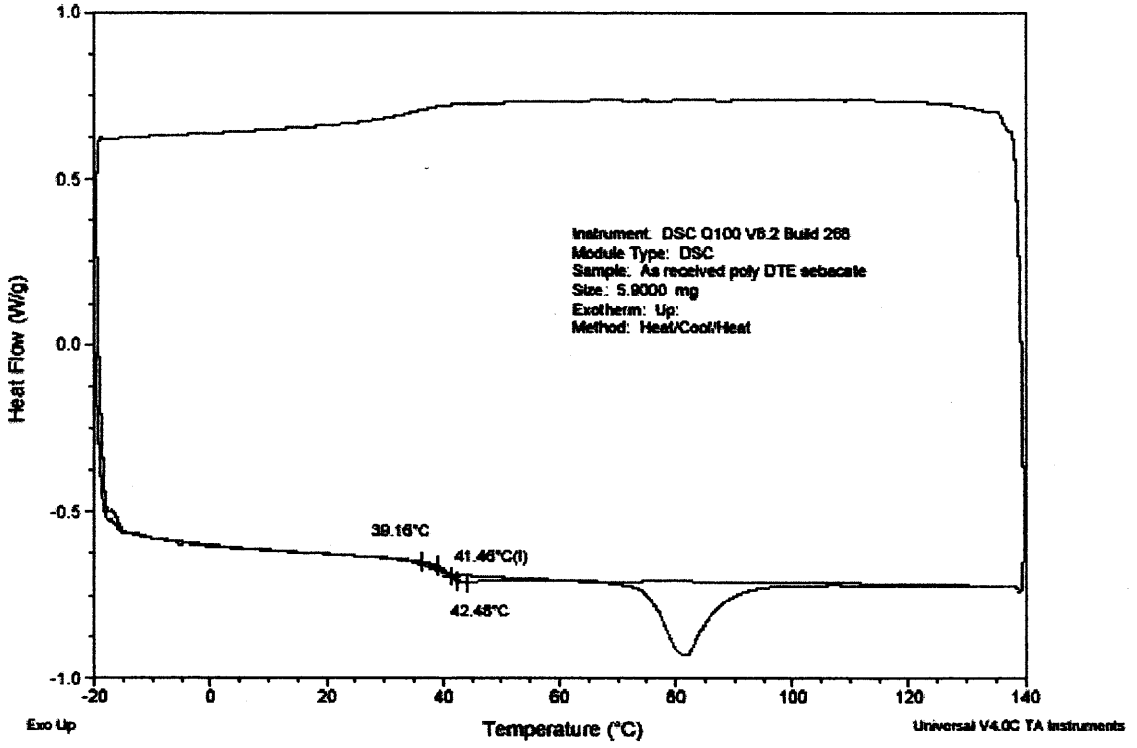

Figure B.7 DSC result of poly DTE sebacate in received form.

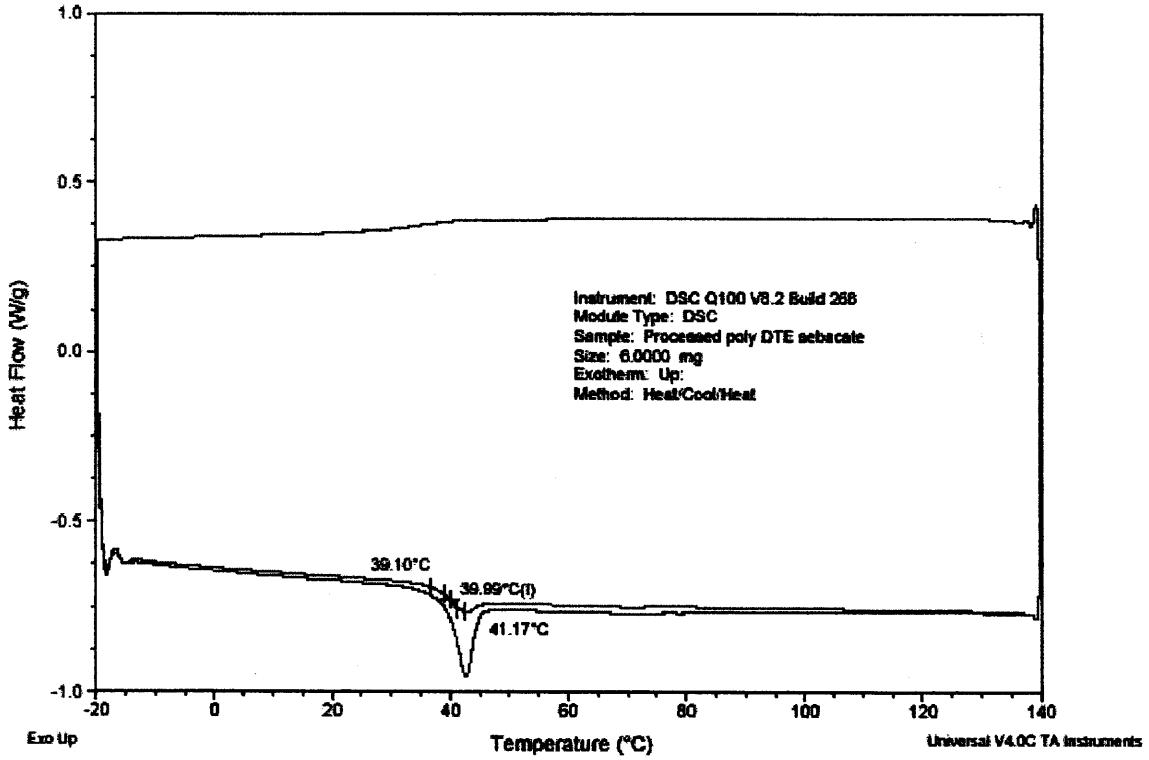

Figure B.8 DSC result of poly DTE sebacate in processed form.

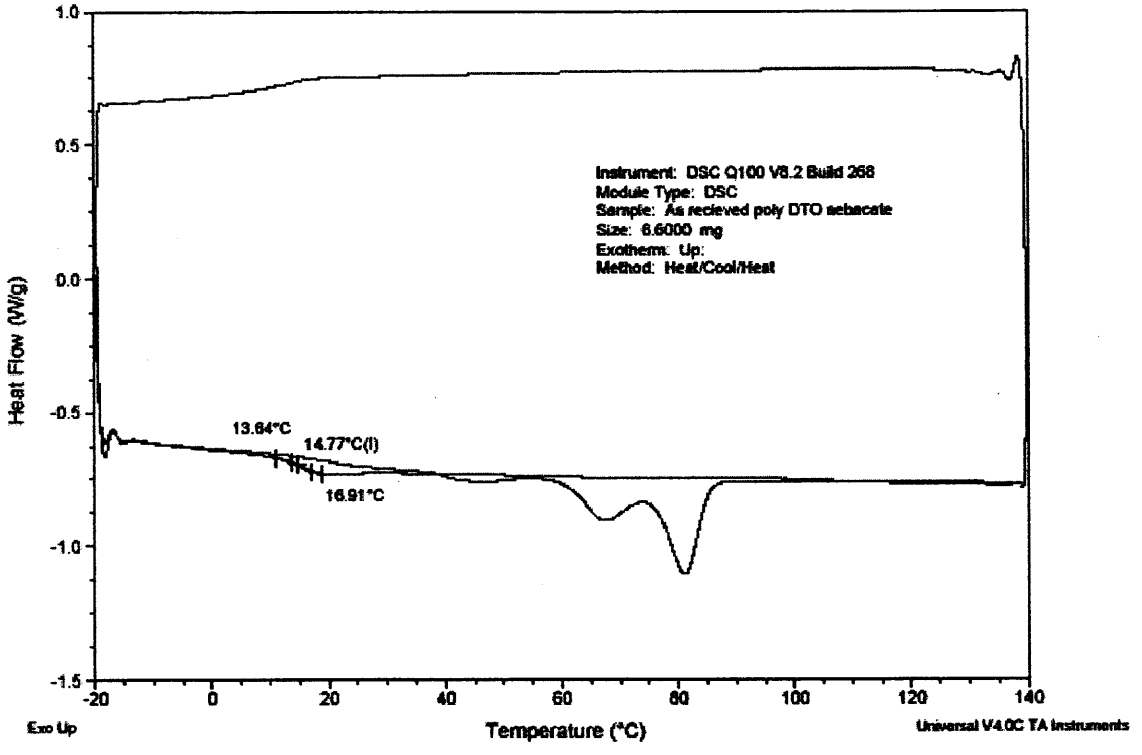

Figure B.9 DSC result of poly DTO sebacate in received form.

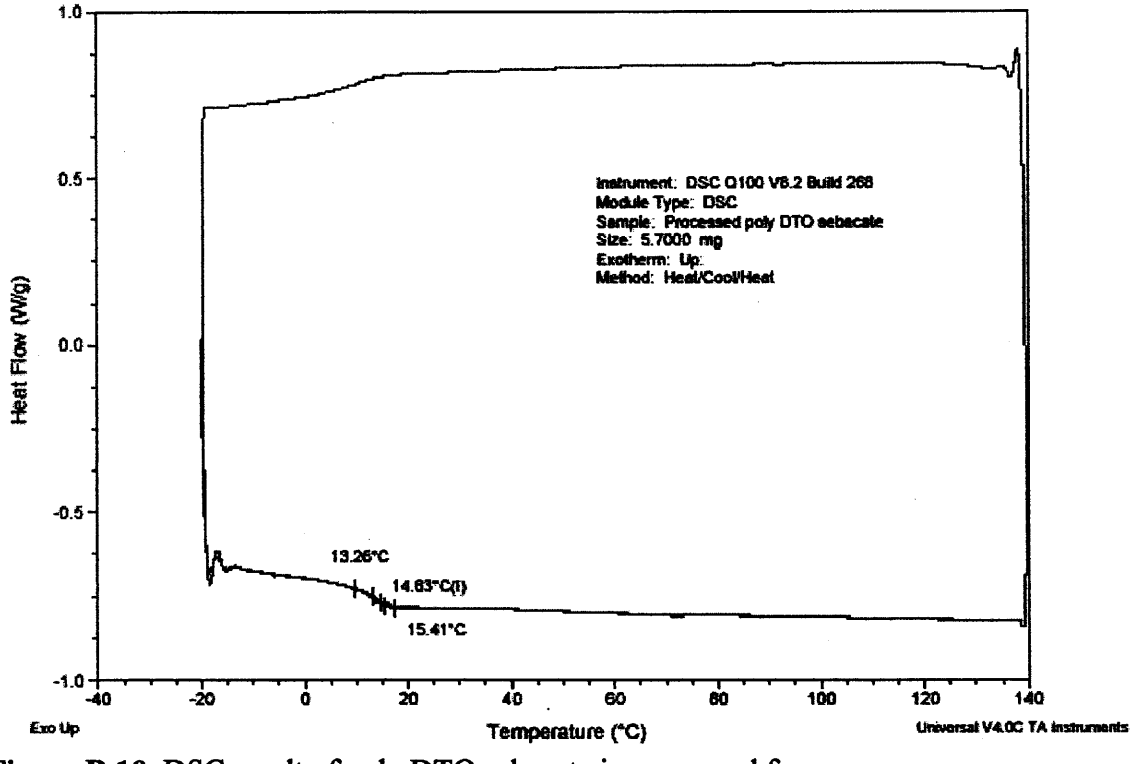

Figure B.10 DSC result of poly DTO sebacate in processed form.

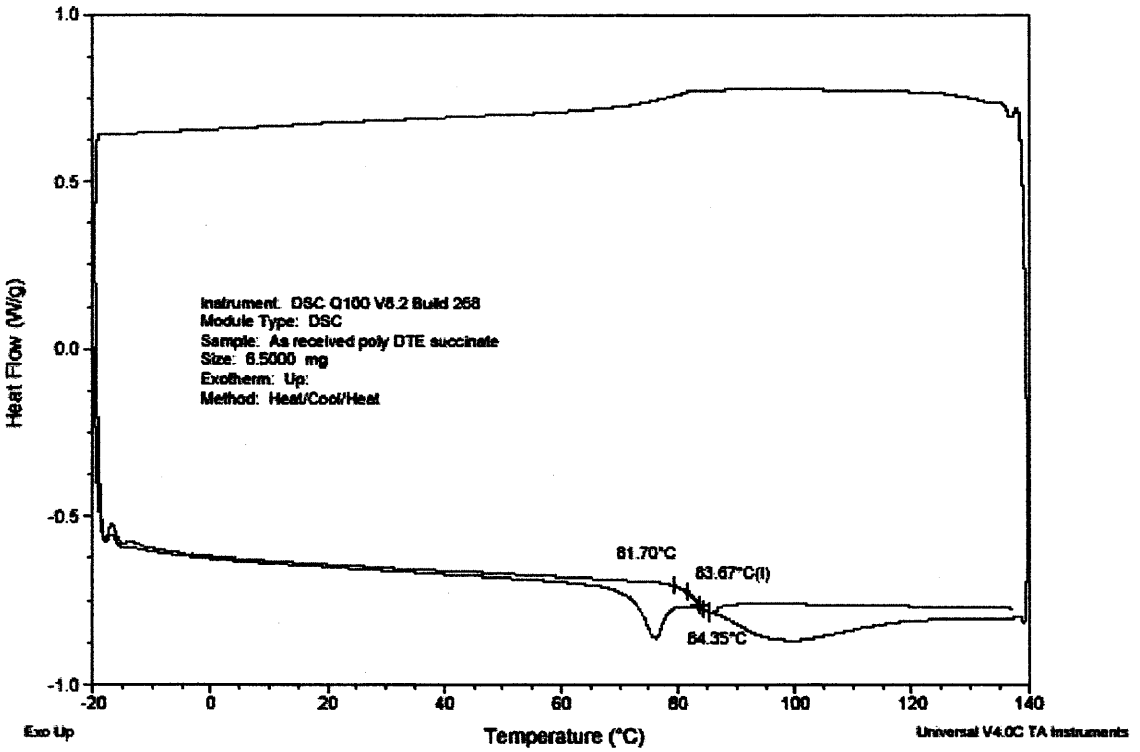

Figure B.11 DSC result of poly DTE succinate in received form.

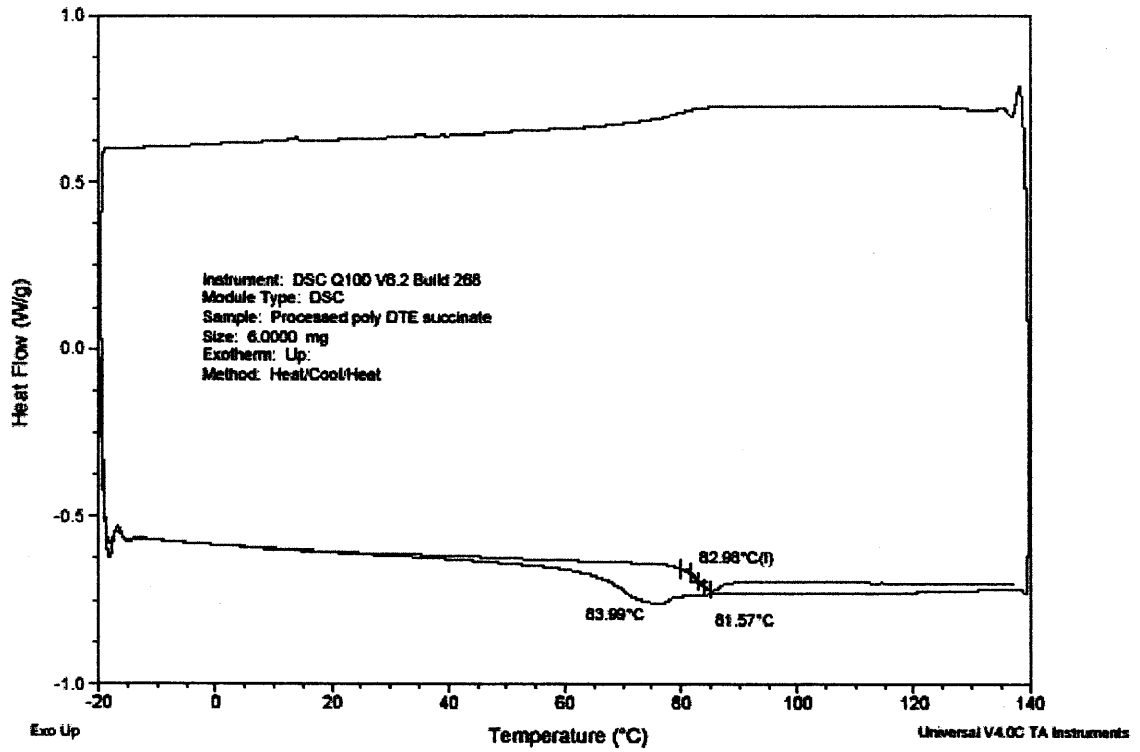

Figure B.12 DSC result of poly DTE succinate in processed form.

REFERENCES

1. http://www.spinalcord.uab.edu/show.asp?durki=21446. Retrieved: May 2005.

2. http://www.ninds.nih.gov/disorders/sci/sci.htm. Retrieved: May 2005.

3. Kandel, E.R., Schwartz, J.H., and Jessell, T.M. (2000). *Principles of Neural Science* (4th edition). US: McGraw-Hill Companies.

4. Schwab, M.E. (2002). Repairing the injured spinal cord. *Science*, 295, 1029-1031.

5. Olson, L. (2002). Medicine: Clearing a path for nerve growth. *Nature*, 416, 589- 590.

6. Olson, L., Cheng. H, Zetterstrom. R.H., Solomin, L., Jansson, L., Gimenez-Llort, L., Hoffer, B.J.,and Perlmann, T. (1998). On CNS repair and protection strategies: novel approaches with implications for spinal cord injury and Parkinson's disease. *Brain Research Reviews*, 26, 302-5.

7. Olson, L. (1997). Regeneration in the adult central nervous system: Experimental repair strategies. *Nature Medicine*, 3, 1329-1335.

8. Guest, J.D., Rao, A., Olson, L., Bunge, M.B., and Bunge, R.P. (1997). The ability of human Schwann cell grafts to promote regeneration in the transected nude rat spinal cord. *Experimental Neurology*, 148, 502-522.

9. Liu, S., Qu, Y., Stewart, T.J., Howard, M.J., Chakrabortty, S., Holekamp, T.F., McDonald, J.W. (2000). Embryonic stem cells differentiate into oligodendrocytes and myelinate in culture and after spinal cord transplantation. *Proceedings of the National Academy of Sciences of the United States of America (PNAS)*, 97, 6126-6131.

10. Hofstetter, C.P., Holmstrom, N.A.V., Lilja, J.A., Schweinhardt, P., Hao, J.X., Spenger, C., Wiesenfeld-Hallin, Z., Kurpad, S.N., Frisen, J., and Olson, L. (2005). Allodynia limits the usefulness of intraspinal neural stem cell grafts; directed differentiation improves outcome. *Nature Neuroscience*, 8, 346-353.

11. Goh, E.L.K., Ma, D.K., Ming, G.L., and Song, H.J. (2003). Adult neural stem cells and repair of the adult central nervous system. *Journal of Hema-totherapy & Stem Cell Research*, 12, 671-679.

12. Hofstetter, C.P., Schwarz, E.J., Hess, D., Widerfalk, J., E.L., Manira, A., Prockop, D.J., and Olson, L. (2002). Marrow stromal cells form guiding strands in the injured spinal cord and promote recovery. *Proceedings of the National Academy of Sciences of the United States of America*, 99, 2199-2204.

13. Klein, S. and Svendsen, C.N. (2005). Stem cells in the injured spinal cord: reducing the pain and increasing the gain. *Nature Neuroscience*, 8, 259-260.

14. Lepore, A.C. and Fischer I. (2005). Lineage-restricted neural precursors survive, migrate, and differentiate following transplantation into the injured adult spinal cord. *Experimental Neurology*, 194, 230-242.

15. Dezawa, M. (2002). Central and peripheral nerve regeneration by transplantation of Schwann cells and transdifferentiated bone marrow stromal cells. *Anatomical Science International*, 77, 12-25.

16. Novikova, L.N., Novikov, L.N., and Kellerth, J.O. (2003). Biopolymers and biodegradable smart implants for tissue regeneration after spinal cord injury. *Current Opinion in Neurology*, 16, 711-5.

17. Stokols, S. and Tuszynski, M.H. (2004). The fabrication and characterization of linearly oriented nerve guidance scaffolds for spinal cord injury. *Biomaterials*, 25, 5839-46.

18. Novikov, L.N., Novikova, L.N., Mosahebi, A., Wiberg, M., Terenghi, G., and Kellerth, J.O. (2002). A novel biodegradable implant for neuronal rescue and regeneration after spinal cord injury. *Biomaterials*, 23, 3369-76.

19. Zhang, X., Prasad, S., Niyogi, S., Morgan, A., Ozkan, M., and Ozkan, C.S. (2005). Guided neurite growth on patterned carbon nanotubes. *Sensors and Actuators B*, 106, 843-850.

20. Holmes, T.C., de Lacalle, S., Su, X., Liu, G.S., Rich, A., and Zhang, S.G. (2000). Extensive neurite outgrowth and active synapse formation on self-assembling peptide scaffolds. *Proceedings of the National Academy of Sciences of the United States of America (PNAS)*, 97, 6728-33.

21. Teng, Y.D., Lavik, E.B., Qu, X.L., Park, K.I., Ourednik, J., Zurakowski, D., Langer, R., and Snyder, E.Y. (2002). Functional recovery following traumatic spinal cord injury mediated by a unique polymer scaffold seeded with neural stem cells. *Proceedings of the National Academy of Sciences of the United States of America*, 99, 3024-9.

22. Stokols, S. and Tuszynski, M.H. (2004). The fabrication and characterization of linearly oriented nerve guidance scaffolds for spinal cord injury. *Biomaterials*, 25, 5839-46.

23. Yang, F., Murugan, R., Wang, S., and Ramakrishna, S. (2005). Electrospinning of nano/micro scale poly($_{L}$-lactic acid) aligned fibers and their potential in neural tissue engineering. *Biomaterials*, 26, 2603-10.

24. Langer, R. and Vacanti, J.P. (1993). Tissue Engineering. *Science*, 260, 920-6.

25. Lanza, R.P., Langer, R., and Vacanti, J. (2000). *Principles of Tissue Engineering*. US: Elsevier Science.

26. Bourke, S.L. and Kohn, J. (2003). Polymers derived from the amino acid L-tyrosine: polycarbonates, polyarylates and copolymers with poly(ethylene glycol). *Advanced Drug Delivery Reviews*, 55, 447-66.

27. Pulapura, S. and Kohn, J. (1992). Tyrosine-derived polycarbonates - backbone-modified pseudo-poly(amino acids) designed for biomedical applications. *Biopolymers*, 32, 411-417.

28. Ertel, S.I. and Kohn, J. (1994). Evaluation of a series of tyrosine-derived polycarbonates as degradable biomaterials. *Journal of Biomedical Materials Research*, 28, 919-30.

29. Brocchini, S., James, K., Tangpasuthadol, V., and Kohn, J. (1998). Structure-property correlations in a combinatorial library of degradable biomaterials. *Journal of Biomedical Materials Research*, 42, 66-75.

30. Yu, C. and Kohn, J. (1999). Tyrosine-PEG-derived poly(ether carbonate)s as new biomaterials - Part I: Synthesis and evaluation. *Biomaterials*, 20, 253-64.

31. PérezLuna, V.H., Hooper, K.A., Kohn, J., and Ratner, B.D. (1997). Surface characterization of tyrosine-derived polycarbonates. *Journal of Applied Polymer Science*, 63, 1467-79.

32. Seyda, A., Kohn, J., and Arinzeh, T.L. (2003). Effect of the polymeric substratum on the differentiation of human mesenchymal stem cells. The 29th Annual Meeting of the Society for Biomaterials.

33. Godbole, M.S., Seyda, A., Kohn, J., and Arinzeh, T.L. (2004). Surface properties of the substratum affect human mesenchymal stem cell differentiation. The Northeast Bioengineering Conference.

34. Bain, G., Kitchens, D., Yao, M., Huettner, J.E., and Gottlieb, D.I. (1995). Embryonic stem-cells express neuronal properties in-vitro. *Developmental Biology*, 168, 342-57.

35. Gearhart, J. (1998). New potential for human embryonic stem cells. *Science*, 282, 1145-7.

36. Pittenger, M.F., Mackay, A.M., Beck, S.C., Jaiswal, R.K., Douglas, R., Mosca, J.D., Moorman, M.A., Simonetti, D.W., Craig, S., and Marshak, D.R. (1999). Multilineage potential of adult human mesenchymal stem cells. *Science*, 284, 143-7.

37. Ferrari, G., Cusella-De Angelis, G., Coletta, M., Paolucci, E., Stornaiuolo, A., Cossu, G., and Mavilio, F. (1998). Muscle regeneration by bone marrow derived myogenic progenitors. *Science*, 279, 1528-30.

38. Lee, S.H., Lumelsky, N., Studer, L., Auerbach, J.M., and McKay, R.D. (2000). Efficient generation of midbrain and hindbrain neurons from mouse embryonic stem cells. *Nature Biotechnology*, 18, 675-9.

39. Kohyama, J., Abe, H., Shimazaki, T., Koizumi, A., Nakashima, K., Gojo, S., Taga, T., Okano, H., Hata, J., and Umezawa, A. (2001). Brain from bone: Efficient "meta-differentiation" of marrow stroma-derived mature osteoblasts to neurons with Noggin or a demethylating agent. *Differentiation*, 68, 235-44.

40. Fraichard, A., Chassande, O., Bilbaut, G., Dehay, C., Savatier, P., and Samarut, J. (1995). In-vitro differentiation of embryonic stem-cells into gilial-cells and functional-neurons. *Journal of Cell Science*, 108, 3181-8.

41. Guan, K.M., Chang, H., Rolletschek, A., and Wobus, A.M.(2001). Embryonic stem cell-derived neurogenesis - Retinoic acid induction and lineage selection of neuronal cells. *Cell and Tissue Research*, 305, 171-6.

42. Schuldiner, M., Yanuka, O., Itskovitz-Eldor, J., Melton, D.A., and Benvenisty, N. (2000). Effects of eight growth factors on the differentiation of cells derived from human embryonic stem cells. *Proceedings of the National Academy of Sciences of the United States of America (PNAS)*, 97, 11307-12.

43. Strübing, C., Ahnerthilger, G., Shan, J., Wiedenmann, B., Hescheler, J., and Wobus, A.M. (1995). Differentiation of pluripotent embryonic stem-cells into the neuronal lineage in-vitro gives rise to mature inhibitory and excitatory neurons. *Mechanisms of Development*, 53, 275-87.

44. Cho, K.J., Trzaska, K.A., Greco, S.J., McArdle, J., Wang, F.S., Ye, J.H., and Rameshwar, P. (2005). Neurons derived from human mesenchymal stem cells show synaptic transmission and can be induced to produce the neurotransmitter substance P by interleukin-1 alpha. *Stem Cell*, 23, 383-91.

45. Sanchez-Ramos, J., Song, S., Cardozo-Pelaez, F., Hazzi, C., Stedeford, T., Willing, A., Freeman, T.B., Saporta, S., Janssen, W., Patel, N., Cooper, D.R., Sanberg, P.R. (2000). Adult bone marrow stromal cells differentiate into neural cells in vitro. *Experimental Neurology*, 164, 247-56.

46. Kim, B.J., Seo, J.H., Bubien, J.K., and Oh, Y.S. (2002). Differentiation of adult bone marrow stem cells into neuroprogenitor cells in vitro. *NeuroReport*, 13, 1185-8.

47. Woodbury, D., Schwarz, E.J., Prockop, D.J., and Black, I.B. (2000). Adult rat and human bone marrow stromal cells differentiate into neurons. *Journal of Neuroscience Research*, 61, 364-70.

48. Black, I.B. and Woodbury, D. (2001). Adult rat and human bone marrow stromal stem cells differentiate into neurons. *Blood Cells Molecules and Diseases*, 27, 632-6.

49. Woodbury, D., Reynolds, K., and Black, I.B. (2002). Adult bone marrow stromal stem cells express germline, ectodermal, endodermal, and mesodermal genes prior to neurogenesis. *Journal of Neuroscience Research*, 96, 908-17.

50. Munoz-Elias, G., Woodbury, D., and Black, I.B. (2003). Marrow stromal cells, mitosis, and neuronal differentiation: Stem cell and precursor functions. *Stem Cells*, 21, 437-48.

51. Deng, W.W., Obrocka, M., Fischer, I., and Prockop, D.J. (2001). In vitro differentiation of human marrow stromal cells into early progenitors of neural cells by conditions that increase intracellular cyclic AMP. *Biochemical and Biophysical Research Communications*, 282, 148-52.

52. Gage, F.H. (2000). Mammalian neural stem cells. *Science*, 287, 1433-8.

53. Yang, F., Murugan, R., Ramakrishna, S., Wang, X., Ma, Y.X., and Wang, S. (2004). Fabrication of nano-structured porous PLLA scaffold intended for nerve tissue engineering. *Biomaterials*, 25, 1891-1900.

54. Qian, L.C. and Saltzman, W.M. (2004). Improving the expansion and neuronal differentiation of mesenchymal stem cells through culture surface modification. *Biomaterials*, 25, 1331-7.

55. http://www.fristtenangstroms.com/faq/DoINeed.html. Retrieved date: June 2005.

56. Jaiswal, N., Haynesworth, S.E., Caplan, A.I., and Bruder, S.P. (1997). Osteogenic differentiation of purified, culture-expanded human mesenchymal stem cells in vitro. *Journal of Cellular Biochemistry*, 64, 295-312.

57. Jaffe, M., Ophir, Z., Collins, G., Recber, A., Yoo, S.U., and Rafalko, J.Y. (2003), Process-structure-property relationships of erodable polymeric biomaterials: II – long range order in poly (desaminotyrosyl arylates). *Polymer*, 44, 6033-6042.

58. Kang, I.K., Ito, Y., Sisido, M., and Imanishi, Y. (1989), Attachment and growth of fibroblast cells on polypeptide derivatives. *Journal of Biomaterial Research*, 23, 223-239.

59. Tamada, Y. and Ikada, Y. (1994). Fibroblast growth on polymer surfaces and biosynthesis of collagen. *Journal of Biomaterial Research*, 28, 783-789.

60. van Wachem, P.B., Hogt, A.H., Beugeling, T., Feijen, J., Bantjes, A., Detmers, J.P., and van Aden, W.G. (1987). Adhesion of cultured human-endothelial cells onto methacrylate polymers with varying surface wettability and charge. *Biomaterials*, 8, 323-328.

61. Ertel, S.I., Ratner, B.D., and Horbett, T.A. (1990). Radiofrequency plasma deposition of oxygen-containing films on polystyrene and poly (ethylene-terephthalate) substrates improves endothelial-cell growth. *Journal of Biomedical Materials Research*, 24, 1637-1659.

62. Ertel, S.I., Chilkoti, A., Horbett, T.A., and Ratner, B.D. (1991). Endothelial-cell growth on oxygen-containing films deposited by radiofrequency plasmas – the role of surface carbonyl groups. *Journal of Biomaterials Science- Polymer Research*, 3, 163-183.

63. Valentini, R.F., Vargo, T.G., Gardella Jr, J.A., and Aebischer, P. (1992). Electrically charged polymeric substrates enhances nerve fiber outgrowth in vitro. *Biomaterials*, 13, 183-90.

64. Brocchini, S., James, K., Tangpasuthadol, V., and Kohn, J. (1997), A combinatorial approach for polymer design. *Journal of American Chemical Society*, 119, 4553-4.

65. Longhurst, C.M. and Jennings, L.K. (1998), Integrin-mediated signal transduction. *Cellular and Molecular Life Science*, 54, 514-526.

66. Garcia, A.J., Vega, M.D., and Boettiger, D. (1999). Modulation of cell proliferation and differentiation through substrate-dependent changes in fibronectin conformation. *Molecular Biology*, 10, 785-98.

67. Ryan, P.L., Foty, R.A., Kohn, J., and Steinberg, S. (2001). Tissue spreading on implantable substrates is a competitive outcome of cell-cell vs. cell-substratum adhesivity. *Proceeding of National Academic Society*, 98, 4323-7.